Journal of
Mechanics of
Materials and Structures

NONLINEAR DYNAMIC RESPONSE OF AN ACCELERATING COMPOSITE ROTOR BLADE USING PERTURBATIONS

Mehrdaad Ghorashi and Fred Nitzsche

Volume 4, Nº 4 April 2009

mathematical sciences publishers

JOURNAL OF MECHANICS OF MATERIALS AND STRUCTURES
Vol. 4, No. 4, 2009

NONLINEAR DYNAMIC RESPONSE OF AN ACCELERATING COMPOSITE ROTOR BLADE USING PERTURBATIONS

MEHRDAAD GHORASHI AND FRED NITZSCHE

The general nonlinear intrinsic differential equations of a composite beam are solved in order to obtain the elastodynamic response of an accelerating rotating hingeless composite beam. The solution utilizes the results of the linear variational asymptotic method applied to cross-sectional analysis. The integration algorithm implements the finite difference method in order to solve the transient form of the nonlinear intrinsic differential equations. The motion is analyzed since the beam starts rotating from rest, until it reaches the steady state condition. It is shown that the transient solution of the nonlinear dynamic formulation of the accelerating rotating beam converges to the steady state solution obtained by an alternative integration algorithm based on the shooting method. The effects of imposing perturbations on the steady state solution have also been analyzed and the results are shown to be compatible with those of the accelerating beam. Finally, the response of a nonlinear composite beam with embedded anisotropic piezocomposite actuators is illustrated. The effect of activating actuators at various directions on the steady state forces and moments generated in a rotating beam has been analyzed. These results can be used in controlling the nonlinear elastodynamic response of adaptive rotating beams.

A list of symbols can be found starting on page 713.

1. Introduction

The helicopter with its ability to take-off and land vertically is a crucial means of aerial transportation. Expanding the domain of application of helicopters, however, face a few serious constraints. Among them is the relatively poor ride quality due to severe vibration and noise. Vibration can reduce the fatigue life of structural components and hence increase the operating costs. Furthermore, environmental consequences of noise and vibration have limited the range of application and the velocity of helicopters. That is why reducing noise and vibration is a major goal in the design of helicopters.

Analysis of rotating blades can be performed using three-dimensional finite element method (FEM) models. However, modeling initially twisted and curved active helicopter rotor blades using three-dimensional FEM is extremely expensive. Also, for preliminary design and for control synthesis, this approach is quite computationally intensive. As an alternative, and since a helicopter rotor blade is a slender structural member, one may model it as a thin-walled composite beam.

In the past two decades, research has focused on the analysis of anisotropic composite beams using the variational asymptotic method (VAM), an excellent review of which can be found in [Hodges 2006]. VAM, as a powerful method for analyzing thin-walled beams made of composites was first introduced

Keywords: rotating beam, intrinsic differential equations of a beam, accelerating beam, steady state solution, variational asymptotic method (VAM), embedded actuators.

Ghorashi gratefully acknowledges an Alexander Graham Bell Canada Graduate Scholarship Award by the Natural Science and Engineering Research Council of Canada, and the J. Y. and E. W. Wong Research Award in Mechanical/Aerospace Engineering.

in [Berdichevskii 1981]. It is computationally more efficient than a complete three-dimensional model and it starts from the elastic energy functional.

For certain simple cases like isotropic beams with relatively simple cross-sectional geometries, the sectional constants can be calculated in closed form. For complex cross-sections made of composites, a two-dimensional FEM discretization has been introduced which implements the VAM cross-sectional analysis. This FEM code is called the *Variational Asymptotic Beam Sectional* Analysis program (VABS). This concept was introduced in [Hodges et al. 1992] and applied to box and I-beams with initial twist and initial curvature.

The results of the VAM cross-sectional analysis have been validated in [Yu et al. 2002b] and [Yu and Hodges 2004]. VABS solutions have been compared with those of the three-dimensional elasticity solution. Identical results were reported for beams with elliptical and rectangular cross-sections. It has been demonstrated that although the application of VABS is restricted to beam problems, it provides a level of accuracy which is comparable to that of standard three-dimensional finite element codes, but with far smaller computing and processing requirements.

The foundations of the Timoshenko model have been developed in [Yu et al. 2002a]. Also, the inclusion of active elements in the analysis was carried out by Cesnik and his coworkers. In [Cesnik and Shin 1998], an asymptotic formulation for analyzing multicell composite helicopter rotor blades with integral anisotropic active plies was presented.

In [Cesnik et al. 2001], the dynamic characteristics of the active twist rotor (ATR) blades were investigated, both analytically and experimentally. The ATR system is intended for vibration and potentially for noise reduction in helicopters through individual blade control (IBC). The numerical results for the beam torsional loads showed an average error of 20% in magnitude and virtually no difference in phase for the blade frequency response.

Not many papers have discussed the method of solution of the one-dimensional intrinsic equations of a beam. In the solutions presented in [Shang and Hodges 1995] and [Cesnik et al. 2001] the solution is performed in two steps. The first step is to calculate the steady state response. Then, the perturbed motion of the blade about the obtained steady state position is obtained by solving the perturbed steady state equations for small perturbations of variables.

This perturbed steady state solution is, of course, valid in the vicinity of the steady state response. If, however, obtaining the whole dynamics of the beam including its start from static equilibrium and acceleration to full speed and even experiencing some perturbations afterwards is the aim, other solution methods should be sought. The purpose of this paper is to present such an alternative solution. In order to verify the results, the results of this alternative method are compared against those of the perturbed steady state method.

In this paper the beam is assumed to accelerate from its state of rest and reach a constant speed of rotation. Both transient and steady state solutions are obtained. The analysis utilizes the results of the cross-sectional analysis and the solution of the nonlinear intrinsic equations of the beam is performed using finite differences, perturbations and the shooting method. To verify the solution, the resulting solutions are compared against those of the perturbed steady state method. The obtained simulation code is a powerful tool for analyzing the nonlinear response of composite rotor blades; and for the ultimate aim of efficient noise and vibration control of helicopters.

This paper is based on [Ghorashi 2009] and its principal features are:

1. Nonlinear dynamic analysis of passive clamped rotating composite beams (transient and steady state solutions) accelerating from zero to full speed.
2. Analyzing the effect of input perturbations on the response of rotating beams which are already at their steady state. This is an extension to [Ghorashi and Nitzsche 2008] where only the steady state response of rotating beams has been discussed.
3. Nonlinear dynamic analysis of a rotating composite beam with embedded actuators and analyzing the sensitivity of the response of the beam to activating the actuators located at various angles.

2. The intrinsic differential equations

The nonlinear one-dimensional analysis along a rotating beam utilizes the results of the cross-sectional analysis. It results in the generalized stress and strain resultants as well as the one-dimensional displacements. For the case of generalized Timoshenko beam, the nonlinear intrinsic equations of motion are [Hodges 2006]

$$F' + \tilde{K}F + f = \dot{P} + \tilde{\Omega}P \quad \text{and} \quad M' + \tilde{K}M + (\tilde{e}_1 + \tilde{\gamma})F + m = \dot{H} + \tilde{\Omega}H + \tilde{V}P, \tag{1}$$

where the total curvature and twist of the beam are the summation of their initial values and the added curvature and twist as a result of elastic deformation, that is,

$$K = k + \kappa. \tag{2}$$

Here, F and M are column vectors of internal forces and moments, respectively. The first element of F is the axial force and the second and third elements are the shear forces, expressed in the deformed beam basis. Similarly, the first element of M is the twisting moment and the second and third elements are bending moments.

The generalized sectional linear and angular momenta P and H are conjugate to motion variables by derivatives of the kinetic energy function $\mathcal{K}$:

$$P = \left(\frac{\partial \mathcal{K}}{\partial V}\right)^T \quad \text{and} \quad H = \left(\frac{\partial \mathcal{K}}{\partial \Omega}\right)^T. \tag{3}$$

The nonlinear intrinsic kinematical equations of a beam that should be solved together with the preceding equations are [Hodges 2006]

$$V' + \tilde{K}V + (\tilde{e}_1 + \tilde{\gamma})\Omega = \dot{\gamma} \quad \text{and} \quad \Omega' + \tilde{K}\Omega = \dot{\kappa}. \tag{4}$$

The momentum-velocity equations are [Hodges 2006]

$$\begin{Bmatrix} P \\ H \end{Bmatrix} = \begin{bmatrix} \mu\Delta & -\mu\tilde{\bar{\xi}} \\ \mu\tilde{\bar{\xi}} & i \end{bmatrix} \begin{Bmatrix} V \\ \Omega \end{Bmatrix}, \tag{5}$$

where $\mu = \langle\langle \rho \rangle\rangle$ (with $\langle\langle u \rangle\rangle$ defined as $\int_A u\,(1 - x_2k_3 - x_3k_2)\,dx_2\,dx_3$, see below),

$$\xi = \begin{Bmatrix} 0 \\ x_2 \\ x_3 \end{Bmatrix}, \qquad \tilde{\bar{\xi}} = \begin{bmatrix} 0 & -\bar{x}_3 & \bar{x}_2 \\ \bar{x}_3 & 0 & 0 \\ -\bar{x}_2 & 0 & 0 \end{bmatrix}, \qquad i = \langle\langle \rho(\xi^T\xi \cdot \Delta - \xi\xi^T) \rangle\rangle = \begin{bmatrix} i_2 + i_3 & 0 & 0 \\ 0 & i_2 & i_{23} \\ 0 & i_{23} & i_3 \end{bmatrix}. \tag{6}$$

The quantity $(1 - x_2k_3 - x_3k_2)$ appearing in the definition of the averaging operator $\langle\langle \cdot \rangle\rangle$ is the square root of the determinant g of the metric tensor in curvilinear coordinates.

Finally, the two-dimensional analysis results in the warping functions as well as the stiffness matrix used in the constitutive equations

$$\begin{Bmatrix} \gamma \\ \kappa \end{Bmatrix} = \underbrace{\begin{bmatrix} R & Z \\ Z^T & T \end{bmatrix}}_{S^{-1}} \begin{Bmatrix} F \\ M \end{Bmatrix}, \qquad \begin{Bmatrix} F \\ M \end{Bmatrix} = \underbrace{\begin{bmatrix} A & B \\ B^T & D \end{bmatrix}}_{S} \begin{Bmatrix} \gamma \\ \kappa \end{Bmatrix}. \tag{7}$$

Equations (1), (2), (4), (5), and $(7)_1$ form a system of twelve nonlinear partial differential equations and fifteen algebraic equations. They have a total of nine unknown vectors: $F, M, V, \Omega, P, H, \gamma, \kappa$, and K, at every node along the beam and at every instant of time. In what follows, these equations are solved using the perturbation method as well as finite differences in time and space.

3. Derivation of the generic nonlinear term

Figure 1 illustrates a beam discretized by N nodes along its span. The corresponding finite difference space-time grid presentation is seen in Figure 2. For a generic variable $\phi(x,t)$, we use the convention

$$\phi_i = \phi(x,t), \tag{8}$$

where i is the beam node number corresponding to the coordinate x. At the points neighboring (x,t) in Figure 2, the same variable can be expressed as

$$\phi_{i+1} = \phi(x+\Delta x, t), \qquad \phi_i^+ = \phi(x, t+\Delta t), \qquad \phi_{i+1}^+ = \phi(x+\Delta x, t+\Delta t), \tag{9}$$

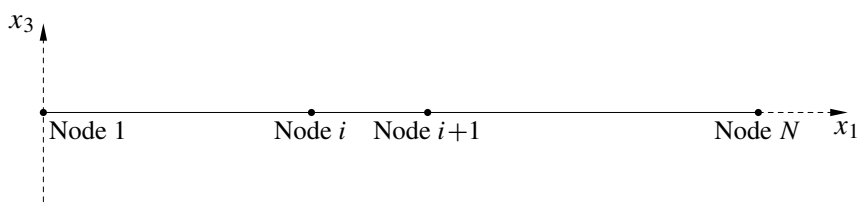

Figure 1. Nodes along the beam and the coordinate system of the undeformed beam.

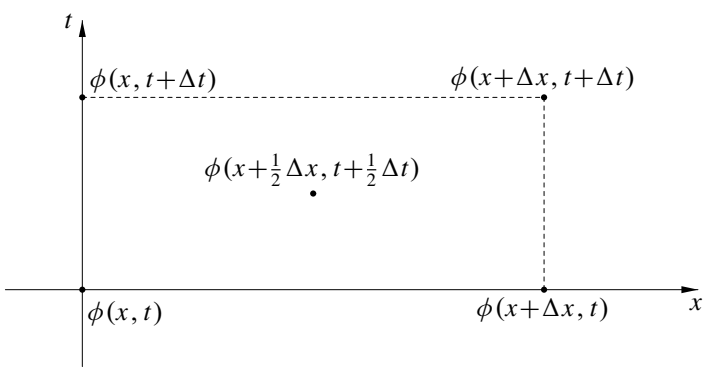

Figure 2. Time-space grid for the numerical solution of a partial differential equation.

where the superscript + refers to the next time step.

Using Taylor series expansions

$$\phi\big(x+\tfrac{1}{2}\Delta x, t+\tfrac{1}{2}\Delta t\big)=\phi\big(x, t+\tfrac{1}{2}\Delta t\big)+\phi'\big(x, t+\tfrac{1}{2}\Delta t\big)\times\tfrac{1}{2}\Delta x, \tag{10}$$

$$\phi\big(x, t+\tfrac{1}{2}\Delta t\big)=\phi(x, t)+\dot{\phi}(x, t)\times\tfrac{1}{2}\Delta t, \tag{11}$$

and the notation given in Equations (8) and (9) one obtains

$$\phi\big(x+\tfrac{1}{2}\Delta x, t+\tfrac{1}{2}\Delta t\big)=\tfrac{1}{4}(\phi^{+}_{i+1}+\phi^{+}_{i}+\phi_{i+1}+\phi_{i})+O(\Delta x^2, \Delta t^2), \tag{12}$$

$$\phi'\big(x+\tfrac{1}{2}\Delta x, t+\tfrac{1}{2}\Delta t\big)=\frac{1}{2\Delta x}(\phi^{+}_{i+1}-\phi^{+}_{i}+\phi_{i+1}-\phi_{i})+O(\Delta x^2, \Delta t^2), \tag{13}$$

$$\dot{\phi}\big(x+\tfrac{1}{2}\Delta x, t+\tfrac{1}{2}\Delta t\big)=\frac{1}{2\Delta t}(\phi^{+}_{i+1}-\phi_{i+1}+\phi^{+}_{i}-\phi_{i})+O(\Delta x^2, \Delta t^2). \tag{14}$$

Equations (12)–(14) provide the second-order approximate finite difference expressions for a variable and its derivatives with respect to time and space. They were used in [Ghorashi 1994] and [Esmailzadeh and Ghorashi 1997] to solve a moving load problem. In what follows, Equations (12)–(14) will be used in order to convert the system of nonlinear partial differential equations (1) and (4) into a set of difference equations.

Consider a generic nonlinear vector term $\tilde{\phi}\lambda$ with scalar components $\phi_m\lambda_n$ $(m=1:3,\ n=1:3)$. One may use perturbations in time and space in order to express these components in terms of the nodal values of variables ϕ_m and λ_n. For the perturbations in space, $\phi^{+}_{m,i+1}=\phi^{+}_{m,i}+\check{\phi}_{m,i+1}$. Similarly, for the perturbations in time, $\phi^{+}_{m,i}=\phi_{m,i}+\hat{\phi}_{m,i}$. Therefore,

$$\phi_m\lambda_n=\tfrac{1}{16}(3\phi_{m,i}+2\hat{\phi}_{m,i}+\check{\phi}_{m,i+1}+\phi_{m,i+1})(3\lambda_{n,i}+2\hat{\lambda}_{n,i}+\check{\lambda}_{n,i+1}+\lambda_{n,i+1}). \tag{15}$$

For small perturbations, (15) reduces to [Ghorashi 2009]

$$\begin{aligned}\phi_m\lambda_n=\tfrac{1}{16}\big[(\phi^{+}_{m,i+1}+\phi^{+}_{m,i})(\lambda_{n,i+1}+3\lambda_{n,i})+(\lambda^{+}_{n,i+1}+\lambda^{+}_{n,i})(\phi_{m,i+1}+3\phi_{m,i})\big]\\ +\tfrac{1}{16}(\phi_{m,i+1}\lambda_{n,i+1}+\phi_{m,i+1}\lambda_{n,i}+\phi_{m,i}\lambda_{n,i+1}-3\phi_{m,i}\lambda_{n,i}).\end{aligned} \tag{16}$$

This is the equation for the generic nonlinear term.

4. The finite difference formulation and solution algorithm

Using (16) for all of the nonlinear terms in (1), and (4), one obtains

$$A_i q^{+}_{i}+B_i q^{+}_{i+1}=J_i, \tag{17}$$

where the right-hand side contains the currently known quantities, the column state vector

$$q=\big[F_1\ F_2\ F_3\ M_1\ M_2\ M_3\ V_1\ V_2\ V_3\ \Omega_1\ \Omega_2\ \Omega_3\ P_1\ P_2\ P_3\ H_1\ H_2\ H_3\ \gamma_{11}\ 2\gamma_{12}\ 2\gamma_{13}\ \kappa_1\ \kappa_2\ \kappa_3\big]^T \tag{18}$$

has 24 elements, the A_i and B_i are 24×24 matrices and q_i and the J_i are column vectors. The expressions for A_i, B_i, and J_i are given in the Appendix.

Equation (17) is composed of 24 algebraic equations with 48 unknowns and as such it is not solvable on its own. To solve the problem, one should utilize initial and boundary conditions as was done for a similar formulation in [Ghorashi 1994] and [Esmailzadeh and Ghorashi 1997]. Using (17) we have

$$q_1^+ = M_{N-1}^{\text{tot}} \cdot q_N^+ + T_{N-1}^{\text{tot}}, \tag{19}$$

where $M_{N-1}^{\text{tot}} = a_1 a_2 a_3 a_4 \cdots a_{N-1}$ and $T_{N-1}^{\text{tot}} = b_1 + a_1 b_2 + a_1 a_2 b_3 + \cdots + a_1 a_2 a_3 \cdots a_{N-2} b_{N-1}$ with $a_i = -A_i^{-1} B_i$ and $b_i = A_i^{-1} J_i$, respectively.

For a hingeless beam with the root (that is, node 1) on the axis of rotation, the boundary conditions at the root are

$$V = \begin{Bmatrix} 0 \\ 0 \\ 0 \end{Bmatrix}, \qquad \Omega = \begin{Bmatrix} 0 \\ 0 \\ \Omega_3 \end{Bmatrix} \tag{20}$$

and at the tip (node N)

$$F = \begin{Bmatrix} 0 \\ 0 \\ 0 \end{Bmatrix}, \qquad M = \begin{Bmatrix} 0 \\ 0 \\ 0 \end{Bmatrix}. \tag{21}$$

By implementing (20) and (21) in (19), the latter equation can be solved for the remainder of the unknowns at the root and at the tip of the beam. Then, (17) can be used to calculate the state vectors at all intermediate nodes.

5. Case studies

5.1. ***The isotropic rectangular solid model.*** Figure 3 illustrates a prismatic beam having a solid rectangular section made of a homogeneous isotropic material for which

$$E = 1.792 \times 10^{13}\,\text{N/m}^2, \quad \upsilon = 0.3, \quad A = 0.02\,\text{m}^2, \quad \rho = 1770\,\text{kg/m}^3. \tag{22}$$

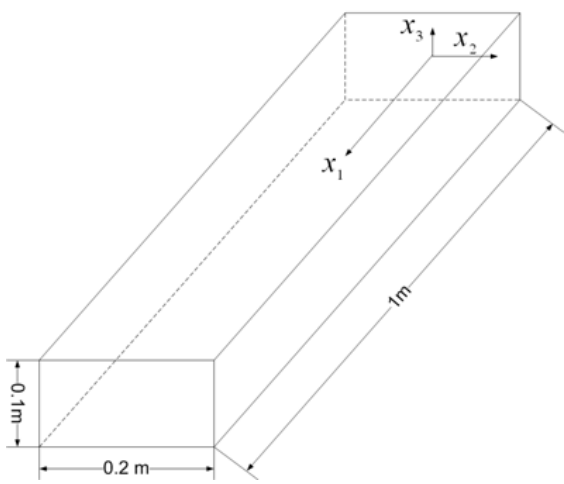

Figure 3. The geometry of the rotating beam and the coordinate system.

Using VABS one obtains

$$i = \begin{bmatrix} 8.333 & 0 & 0 \\ 0 & 1.6667 & 0 \\ 0 & 0 & 6.6667 \end{bmatrix} \times 10^{-5} \times 1770 \tag{23}$$

and

$$S = \begin{bmatrix} 0.358 \times 10^{12} & 0 & 0 & 0 & 0 & 0 \\ 0 & 0.1373 \times 10^{12} & 0 & 0 & 0 & 0 \\ 0 & 0 & 0.1074 \times 10^{12} & 0 & 0 & 0 \\ 0 & 0 & 0 & 0.354 \times 10^{9} & 0 & 0 \\ 0 & 0 & 0 & 0 & 0.298 \times 10^{9} & 0 \\ 0 & 0 & 0 & 0 & 0 & 0.119 \times 10^{10} \end{bmatrix}. \tag{24}$$

The beam rotates about x_3 with the variable angular velocity shown in Figure 4. The corresponding moment at the root is also plotted in the same figure. It is observed that when the beam reaches its steady state velocity, this moment converges to zero. This observation is expected since no drag force exists in the model.

Since the most significant force generated in the beam is the axial force F_1, it is beneficial to have an alternative expression for this force in order to be used for verification. Using linear elasticity and Newton's second law of motion one obtains

$$F_1 = \tfrac{1}{2}\rho A \Omega_3^2 (L^2 - x_1^2). \tag{25}$$

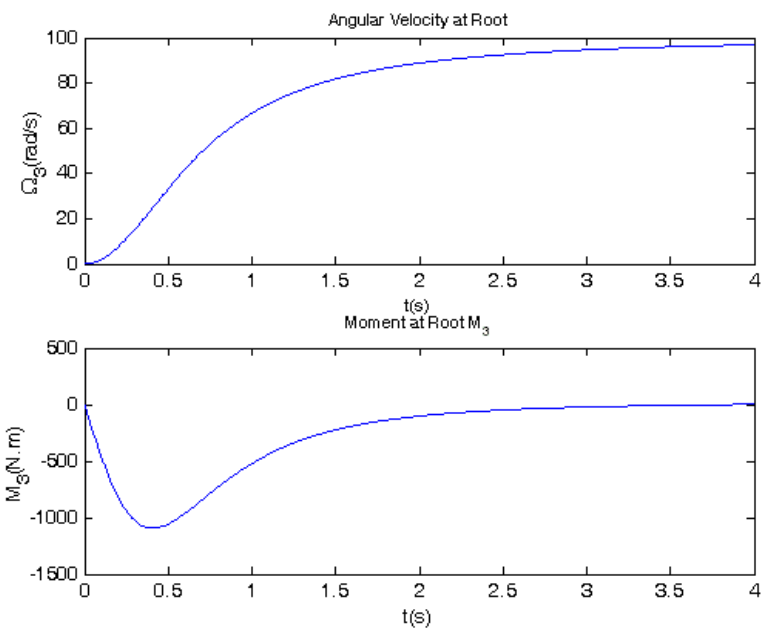

Figure 4. Time history diagram of the angular velocity Ω_3 at the root and the corresponding bending moment at the clamped root.

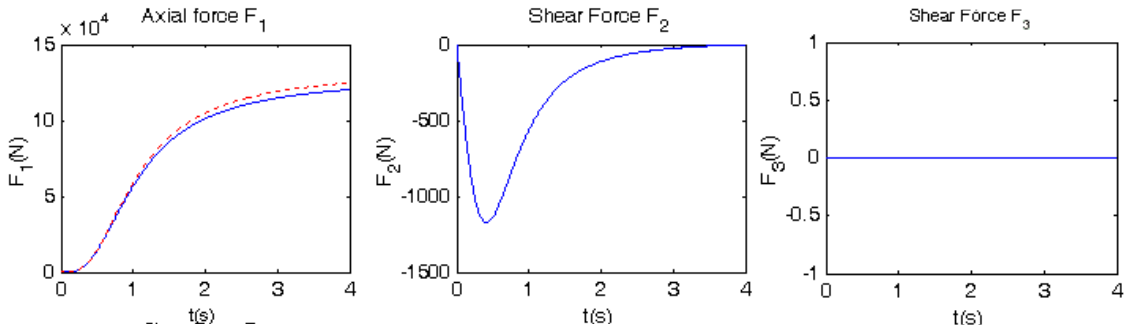

Figure 5. Time history diagram of the internal forces at the midspan (solid lines), and a comparison with the result of (25) (dashed line in left panel).

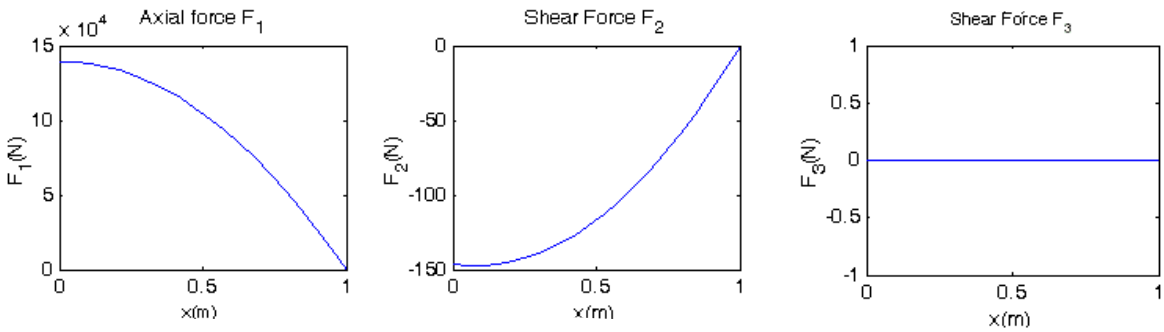

Figure 6. Variation of the internal force components along the beam at $t = 2s$.

Figure 5 illustrates the time history diagram of the induced internal forces at the midspan. It is observed that the measured F_1 is close to that of the approximation of (25). The distributions of the induced internal forces along the span are plotted in Figure 6.

5.2. ***The composite box model.*** The figure illustrates the cross-section of a composite square box beam with constant properties along the beam span and a cross-section of 2.5 cm between midlines. The upper and lower sides are made of four plies of AS4/3506-1 at 45° with the beam axis, and the lateral sides are made of four plies of a typical anisotropic piezocomposite actuator (APA) at −45°. The thickness of each ply is 0.127 mm and the length of the box is $L = 10$ cm. The cross-section of this model was discussed in [Cesnik and Palacios 2003] and the UM/VABS input file for this case is among the examples provided with the software.

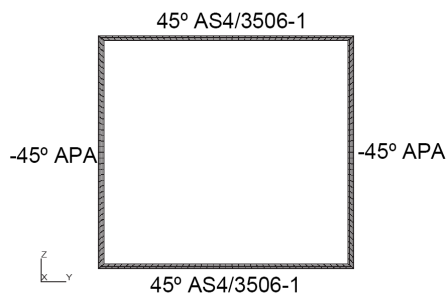

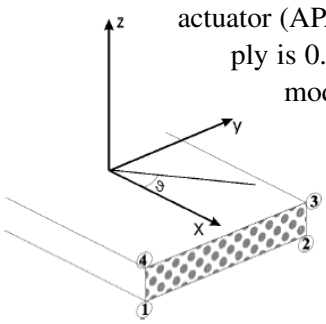

The ply angles mentioned are the angles of fibers with the longitudinal x-axis as shown in the cross-sectional view to the left, which is taken from [Palacios 2005]. The convention for material orientation within the element is also shown.

	E_{11} GPa	E_{22} GPa	G_{12} GPa	G_{23} GPa	ν_{12}	ν_{23}	d_{111} pm/V	d_{112} pm/V	t mm	inter-electrode distance, mm
AS4/3506-1	142	9.8	6.0	4.8	0.3	0.42	—	—	0.127	—
APA	42.2	17.5	5.5	4.4	0.354	0.42	381	−160	0.127	1.143

Table 1. Material properties of active box beam [Cesnik and Palacios 2003].

The material properties are listed in Table 1. It is furthermore assumed that $\rho = 1770\,\text{kg/m}^3$ and $E_{33} = 0.8E_{22}$ and $\nu_{13} = \nu_{23} = \nu_{12}$ [Cesnik and Palacios 2003].

Using these data, the stiffness matrix can be calculated by UM/VABS as

$$S = \begin{bmatrix} 7.977\times10^{5} & -0.9873 & -0.8575 & -1.5056\times10^{3} & -7.3017\times10^{-3} & 1.348\times10^{-3} \\ -0.9873 & 2.5482\times10^{5} & 4.6845\times10^{-3} & -3.897\times10^{-3} & 1.962\times10^{3} & 5.9626\times10^{-5} \\ -0.8575 & 4.6845\times10^{-3} & 2.296\times10^{5} & 1.0716\times10^{-2} & 9.912\times10^{-5} & -2.8055\times10^{2} \\ -1.5056\times10^{3} & -3.897\times10^{-3} & 1.0716\times10^{-2} & 86.95 & 2.1193\times10^{-4} & 1.6532\times10^{-4} \\ -7.3017\times10^{-3} & 1.962\times10^{3} & 9.912\times10^{-5} & 2.1193\times10^{-4} & 90.397 & 3.6091\times10^{-6} \\ 1.348\times10^{-3} & 5.9626\times10^{-5} & -2.8055\times10^{2} & 1.6532\times10^{-4} & 3.6091\times10^{-6} & 79.4434 \end{bmatrix}. \tag{26}$$

Also

$$i = \begin{bmatrix} 9.9555 & 0 & 0 \\ 0 & 4.9777 & 0 \\ 0 & 0 & 4.9777 \end{bmatrix} \times 10^{-9} \times 1770. \tag{27}$$

The cross-sectional area is $5.08 \times 10^{-5}\,\text{m}^2$ and the model has 50 nodes along its span. The beam accelerates from rest to 100 rad/s. Parts of the transient response of the beam from rest to full speed are illustrated in Figures 7 to 9.

6. Steady state solution using the shooting method

The finite difference solution formulated and implemented in Sections 3 and 4 can provide the response of a rotating beam during acceleration to full speed, its convergence to steady state response and also during any existing disturbance that can drive the system out of the steady state response.

In [Ghorashi and Nitzsche 2008] and [Ghorashi 2009] a method for obtaining the steady state response of rotating hingeless beams using the shooting method has been presented. The mathematical basis for

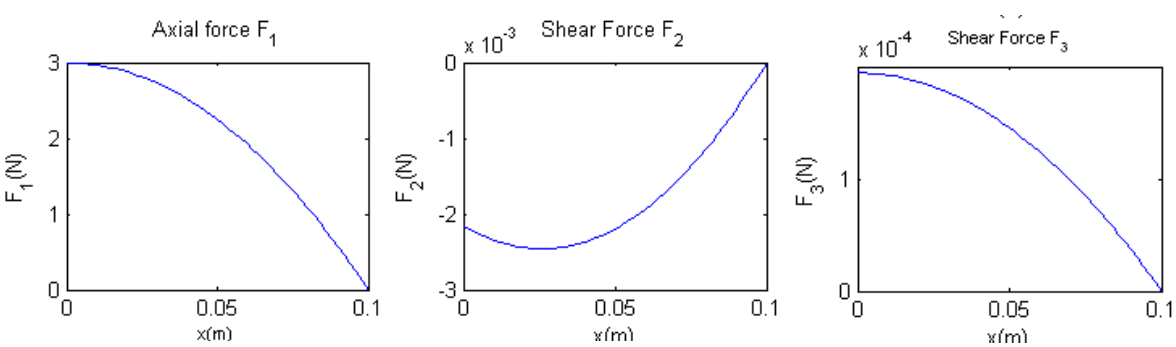

Figure 7. Variation of the internal force components along the beam at $t = 3s$.

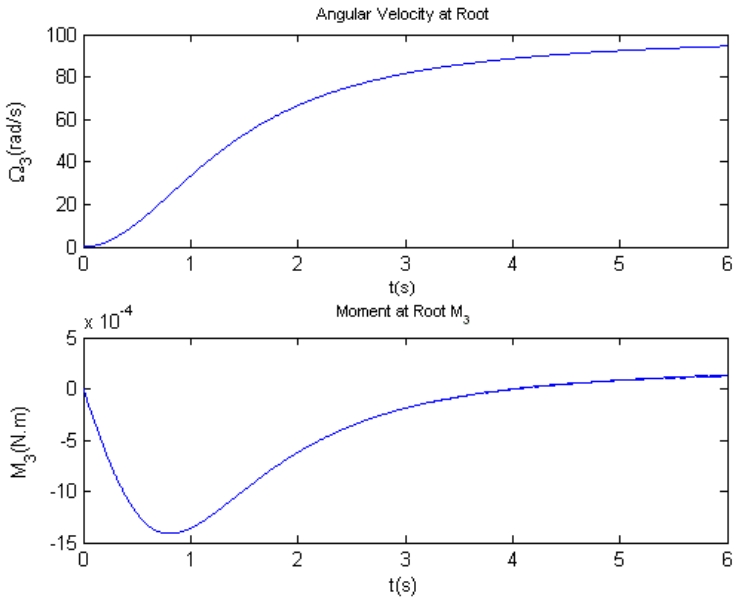

Figure 8. Time history diagram of the angular velocity Ω_3 at the root and the corresponding bending moment at the clamped root.

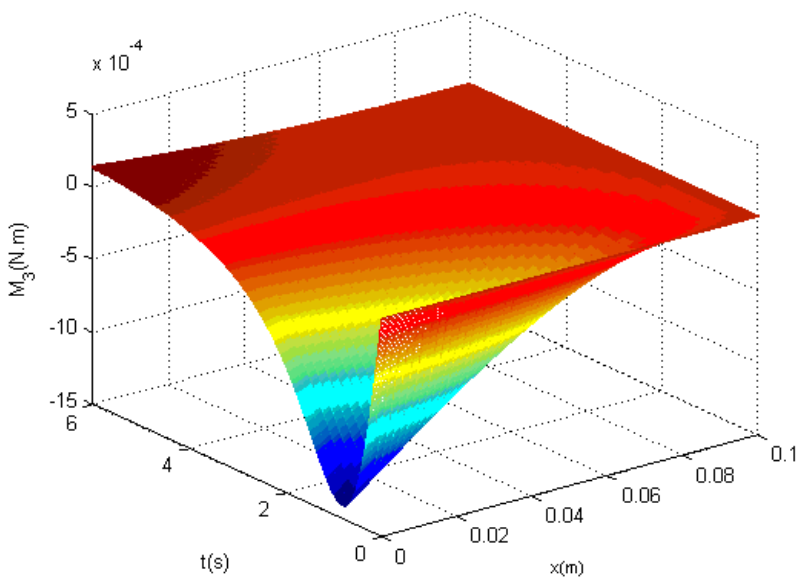

Figure 9. The time-space variation of M_3 at the root.

the method has been discussed in detail in, for example, [Esmailzadeh et al. 1995] and [Zwillinger 1998]. In this section this method is briefly reviewed and in the next section it will be used to provide solutions for the case of perturbed steady state. This perturbed steady state solution has the same logic as the one used in [Shang and Hodges 1995] and [Cesnik et al. 2001] although the mathematical details are different.

The steady state form of the governing equations (1) and (4) are the equations (28), (29), (30), and (31) listed below

$$\begin{aligned} F_1' &= -K_2F_3 + K_3F_2 + \Omega_2P_3 - \Omega_3P_2 - f_1, \\ F_2' &= -K_3F_1 + K_1F_3 + \Omega_3P_1 - \Omega_1P_3 - f_2, \\ F_3' &= -K_1F_2 + K_2F_1 + \Omega_1P_2 - \Omega_2P_1 - f_3, \end{aligned} \tag{28}$$

$$\begin{aligned} M_1' &= -K_2M_3 + K_3M_2 - 2\gamma_{12}F_3 + 2\gamma_{13}F_2 + \Omega_2H_3 - \Omega_3H_2 + V_2P_3 - V_3P_2 - m_1, \\ M_2' &= -K_3M_1 + K_1M_3 - 2\gamma_{13}F_1 + (1+\gamma_{11})F_3 + \Omega_3H_1 - \Omega_1H_3 + V_3P_1 - V_1P_3 - m_2, \\ M_3' &= -K_1M_2 + K_2M_1 - (1+\gamma_{11})F_2 + 2\gamma_{12}F_1 + \Omega_1H_2 - \Omega_2H_1 + V_1P_2 - V_2P_1 - m_3, \end{aligned} \tag{29}$$

$$\begin{aligned} V_1' &= -K_2V_3 + K_3V_2 - 2\gamma_{12}\Omega_3 + 2\gamma_{13}\Omega_2, \\ V_2' &= -K_3V_1 + K_1V_3 + (1+\gamma_{11})\Omega_3 - 2\gamma_{13}\Omega_1, \\ V_3' &= -K_1V_2 + K_2V_1 - (1+\gamma_{11})\Omega_2 + 2\gamma_{12}\Omega_1, \end{aligned} \tag{30}$$

$$\begin{aligned} \Omega_1' &= -K_2\Omega_3 + K_3\Omega_2, \\ \Omega_2' &= -K_3\Omega_1 + K_1\Omega_3, \\ \Omega_3' &= -K_1\Omega_2 + K_2\Omega_1. \end{aligned} \tag{31}$$

These equations form a system of twelve nonlinear ordinary differential equations in terms of the components of F, M, V and Ω. They should be solved together with the hingeless boundary conditions (20) and (21) at the root and the tip of the beam, respectively. The solution would be the nonlinear steady state response of the rotating composite beam.

To solve this problem, the original nonlninear boundary value problem is converted into an initial value problem, by guessing the unknown values of force and moment components at the root. Next, the Runge–Kutta method is used to solve this initial value problem. If this solution satisfies the force and moment boundary conditions at the tip of the beam, the correct solution to the boundary value problem has been obtained. Otherwise, the assumed initial conditions at the root are in error and should be modified.

The modification is performed iteratively by the use of the Newton–Raphson algorithm. The solution of the initial value problem and the update of the initial conditions are repeated until the correct solution to the problem is obtained.

Denote the known (target) values of the boundary conditions at tip of the beam by β_j, where $j = 1, \ldots, 6$. These conditions are related to physical quantities with current (actual) values g_j. These quantities are used for verifying the implemented initial conditions at the root of the beam.

Also, the unknown initial conditions at the root are shown by α_i, where $i = 1, \ldots, 6$. The guessed values of these variables at the root are denoted by α_{i0}. Each g_j at the free end is a function of the adopted values of the initial conditions. Using those guessed values, a corresponding estimation for β_j at the free end is obtained and denoted by β_{j0}

$$g_j(\alpha_{i0}, L) = \beta_{j0}. \tag{32}$$

The proper initial conditions at the root α_i are those for which g_j becomes equal to the known boundary value β_j. The desired g_j can be related to $g_j(\alpha_{i0}, L)$ using the Taylor series expansion

$$g_j(\alpha_i, L) \approx g_j(\alpha_{i0}, L) + \sum_{i=1}^{6} \frac{\partial g_j}{\partial \alpha_i}(\alpha_{i0}, L) \times \Delta\alpha_i. \tag{33}$$

For ideal initial conditions, the left-hand side of Equation (33) is zero. Expanding the rest

$$0 = \begin{Bmatrix} g_1(\alpha_{i0}, L) \\ g_2(\alpha_{i0}, L) \\ g_3(\alpha_{i0}, L) \\ g_4(\alpha_{i0}, L) \\ g_5(\alpha_{i0}, L) \\ g_6(\alpha_{i0}, L) \end{Bmatrix} + \begin{bmatrix} \partial g_1/\partial\alpha_1 & \partial g_1/\partial\alpha_2 & \partial g_1/\partial\alpha_3 & \partial g_1/\partial\alpha_4 & \partial g_1/\partial\alpha_5 & \partial g_1/\partial\alpha_6 \\ \partial g_2/\partial\alpha_1 & \partial g_2/\partial\alpha_2 & \partial g_2/\partial\alpha_3 & \partial g_2/\partial\alpha_4 & \partial g_2/\partial\alpha_5 & \partial g_2/\partial\alpha_6 \\ \partial g_3/\partial\alpha_1 & \partial g_3/\partial\alpha_2 & \partial g_3/\partial\alpha_3 & \partial g_3/\partial\alpha_4 & \partial g_3/\partial\alpha_5 & \partial g_3/\partial\alpha_6 \\ \partial g_4/\partial\alpha_1 & \partial g_4/\partial\alpha_2 & \partial g_4/\partial\alpha_3 & \partial g_4/\partial\alpha_4 & \partial g_4/\partial\alpha_5 & \partial g_4/\partial\alpha_6 \\ \partial g_5/\partial\alpha_1 & \partial g_5/\partial\alpha_2 & \partial g_5/\partial\alpha_3 & \partial g_5/\partial\alpha_4 & \partial g_5/\partial\alpha_5 & \partial g_5/\partial\alpha_6 \\ \partial g_6/\partial\alpha_1 & \partial g_6/\partial\alpha_2 & \partial g_6/\partial\alpha_3 & \partial g_6/\partial\alpha_4 & \partial g_6/\partial\alpha_5 & \partial g_6/\partial\alpha_6 \end{bmatrix} \begin{Bmatrix} \Delta\alpha_1 \\ \Delta\alpha_2 \\ \Delta\alpha_3 \\ \Delta\alpha_4 \\ \Delta\alpha_5 \\ \Delta\alpha_6 \end{Bmatrix}. \tag{34}$$

The Jacobian matrix in Equation (34) includes the sensitivities of the boundary values at the tip with respect to the assumed initial conditions at the root which are

$$\frac{\partial g_j}{\partial \alpha_2}(\alpha_{i0}, L) = \frac{g_j(\alpha_{10}, \alpha_{20} + \epsilon, \alpha_{30}, \alpha_{40}, \alpha_{50}, \alpha_{60}, L) - g_j(\alpha_{10}, \alpha_{20} - \epsilon, \alpha_{30}, \alpha_{40}, \alpha_{50}, \alpha_{60}, L)}{2\epsilon}. \tag{35}$$

So, the best modifications of the initial conditions are

$$\begin{Bmatrix} \Delta\alpha_1 \\ \Delta\alpha_2 \\ \Delta\alpha_3 \\ \Delta\alpha_4 \\ \Delta\alpha_5 \\ \Delta\alpha_6 \end{Bmatrix} = - \begin{bmatrix} \partial g_1/\partial\alpha_1 & \partial g_1/\partial\alpha_2 & \partial g_1/\partial\alpha_3 & \partial g_1/\partial\alpha_4 & \partial g_1/\partial\alpha_5 & \partial g_1/\partial\alpha_6 \\ \partial g_2/\partial\alpha_1 & \partial g_2/\partial\alpha_2 & \partial g_2/\partial\alpha_3 & \partial g_2/\partial\alpha_4 & \partial g_2/\partial\alpha_5 & \partial g_2/\partial\alpha_6 \\ \partial g_3/\partial\alpha_1 & \partial g_3/\partial\alpha_2 & \partial g_3/\partial\alpha_3 & \partial g_3/\partial\alpha_4 & \partial g_3/\partial\alpha_5 & \partial g_3/\partial\alpha_6 \\ \partial g_4/\partial\alpha_1 & \partial g_4/\partial\alpha_2 & \partial g_4/\partial\alpha_3 & \partial g_4/\partial\alpha_4 & \partial g_4/\partial\alpha_5 & \partial g_4/\partial\alpha_6 \\ \partial g_5/\partial\alpha_1 & \partial g_5/\partial\alpha_2 & \partial g_5/\partial\alpha_3 & \partial g_5/\partial\alpha_4 & \partial g_5/\partial\alpha_5 & \partial g_5/\partial\alpha_6 \\ \partial g_6/\partial\alpha_1 & \partial g_6/\partial\alpha_2 & \partial g_6/\partial\alpha_3 & \partial g_6/\partial\alpha_4 & \partial g_6/\partial\alpha_5 & \partial g_6/\partial\alpha_6 \end{bmatrix}^{-1} \begin{Bmatrix} g_1(\alpha_{i0}, L) \\ g_2(\alpha_{i0}, L) \\ g_3(\alpha_{i0}, L) \\ g_4(\alpha_{i0}, L) \\ g_5(\alpha_{i0}, L) \\ g_6(\alpha_{i0}, L) \end{Bmatrix}. \tag{36}$$

The calculated increments are then used to improve the initial guess values

$$\alpha_i = \alpha_{i0} + \Delta\alpha_i. \tag{37}$$

Now the whole procedure can be repeated using the new set of assumed initial conditions (37). By repeating this algorithm, the unknown initial conditions will gradually improve. The procedure can be terminated when a properly defined convergence criterion like $\sum_{i=1}^{6} |g_j(\alpha_i, L)| < \epsilon$ is satisfied. At this instant, the correct initial conditions and consequently, the correct steady state response of the beam have been obtained with enough accuracy.

6.1. ***The isotropic rectangular solid model.*** The isotropic rectangular solid model introduced before is considered again. A root angular velocity of $\Omega_3 = 100$ rad/s is applied and the steady state response of the beam is sought.

Figure 10 illustrates the corresponding steady state distribution of the axial force F_1, which is the dominant force, along the beam. To plot this figure, the shooting method and the finite-difference method (FDM), discussed in Sections 3 and 4 were used. It is observed that the transient finite difference solution

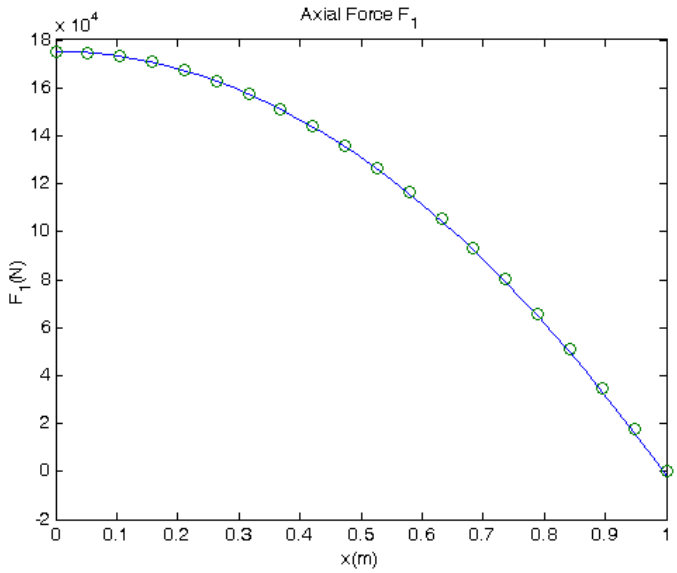

Figure 10. The steady state values of the internal force F_1 along the beam using the shooting method (solid line) the FDM (circles).

has converged to the steady state response obtained by the shooting method and that the two steady state solutions are almost identical.

7. Perturbed steady state analysis

Consider a rotating beam already in its steady state condition. Now the response of this beam to a small input perturbation is of interest. Referring to Figure 2, for every dependent variable one may write

$$\phi\left(x+\tfrac{1}{2}\Delta x, t+\tfrac{1}{2}\Delta t\right)=\phi_{ss}\left(x+\tfrac{1}{2}\Delta x\right)+\phi_p\left(x+\tfrac{1}{2}\Delta x, t+\tfrac{1}{2}\Delta t\right). \tag{38}$$

That is, the whole solution for the variable of interest is the summation of its steady state value and the perturbations about the steady state. Using (38) for the two variables ϕ_m and λ_n, the perturbation part of the generic nonlinear term $\phi_m\lambda_n$ can be written as

$$\begin{aligned}&\left\{\phi_m\left(x+\tfrac{1}{2}\Delta x, t+\tfrac{1}{2}\Delta t\right)\lambda_n\left(x+\tfrac{1}{2}\Delta x, t+\tfrac{1}{2}\Delta t\right)\right\}_p\\&\quad=\phi_{m,ss}\left(x+\tfrac{1}{2}\Delta x\right)\lambda_{n,p}\left(x+\tfrac{1}{2}\Delta x, t+\tfrac{1}{2}\Delta t\right)+\phi_{m,p}\left(x+\tfrac{1}{2}\Delta x, t+\tfrac{1}{2}\Delta t\right)\lambda_{n,ss}\left(x+\tfrac{1}{2}\Delta x\right).\end{aligned} \tag{39}$$

Or, using (12),

$$\begin{aligned}&\left\{\phi_m\left(x+\tfrac{1}{2}\Delta x, t+\tfrac{1}{2}\Delta t\right)\lambda_n\left(x+\tfrac{1}{2}\Delta x, t+\tfrac{1}{2}\Delta t\right)\right\}_p\\&\quad=\tfrac{1}{8}\left[(\phi_{m,ss,i+1}+\phi_{m,ss,i})(\lambda^+_{n,p,i+1}+\lambda^+_{n,p,i}+\lambda_{n,p,i+1}+\lambda_{n,p,i})\right]\\&\qquad+\tfrac{1}{8}\left[(\lambda_{n,ss,i+1}+\lambda_{n,ss,i})(\phi^+_{m,p,i+1}+\phi^+_{m,p,i}+\phi_{m,p,i+1}+\phi_{m,p,i})\right].\end{aligned} \tag{40}$$

Implementation of (40) puts the dynamic governing Equations (1), (2), (4), (5) and $(7)_1$ into matrix form:

$$A_{ss,i}q^{+}_{p,i} + B_{ss,i}q^{+}_{p,i+1} = J_{ss,i}, \tag{41}$$

where q_p contains the perturbations of the variables given in (18). The rest of the solution is similar to that of Section 4.

It should be pointed out that the present method provides solutions only in the vicinity of the steady state solution. Whereas, the previously mentioned FDM obtains solutions for the whole dynamics of the accelerating beam up to full speed.

7.1. ***The isotropic rectangular solid model.*** The isotropic rectangular solid model introduced before is considered. The steady state angular velocity is $\Omega_3 = 93.5$ rad/s and a root angular velocity perturbation of

$$\Omega_{3,p,1} = \sin(93.5t)\ \text{rad/s} \tag{42}$$

is applied at the root (that is, at node number 1) as shown in Figure 11. The implementation of the above-mentioned method results in the perturbations of all of the dependent variables.

Having calculated the perturbations of all of the dependent variables, one may now use (38) in order to get the complete dynamic response. In Figures 11 to 14, the steady state values are plotted with solid lines until $t = 2.667$ s. At this instant, the angular velocity perturbation given by (42) is applied at the root of the beam. In Figures 12 to 14, the effects of this perturbation on bending moment and force components at the root have been illustrated with solid lines.

Alternatively, one may use the algorithm discussed in Section 4 for an accelerating beam to do the same job. In this case, the beam starts to rotate from rest and at $t = 2.667$ s when the beam has an

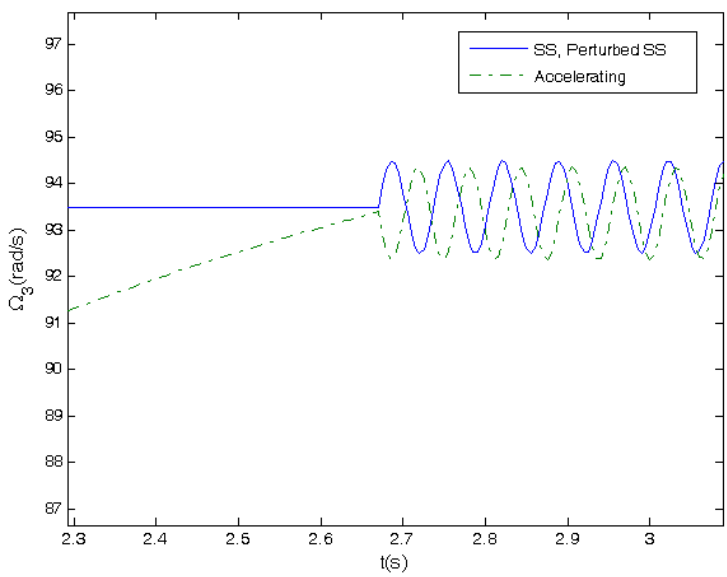

Figure 11. Steady state, accelerating, and perturbed steady state angular velocities at the root.

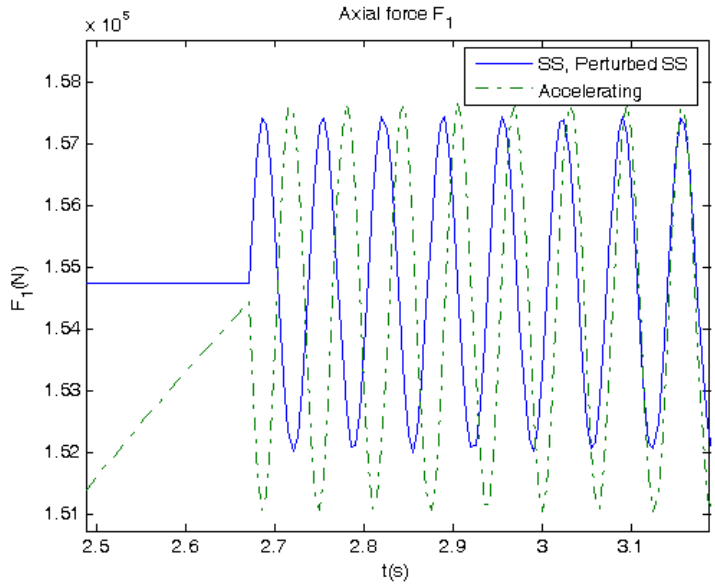

Figure 12. Steady state, accelerating and perturbed axial force at the root.

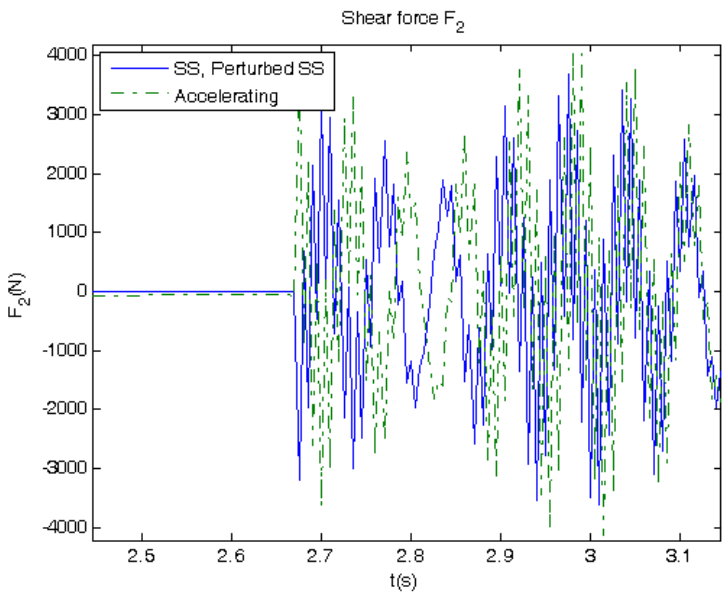

Figure 13. Steady state, accelerating and perturbed shear force at the root.

angular velocity of 93.5 rad/s, the perturbation shown in (42) is applied. In Figures 12 to 14 the results corresponding to this algorithm are plotted with dash-dotted lines.

It can be observed that the predictions of the perturbed steady state method discussed in this section are close to those of the accelerating beam presented in Section 4. The results of such an analysis can

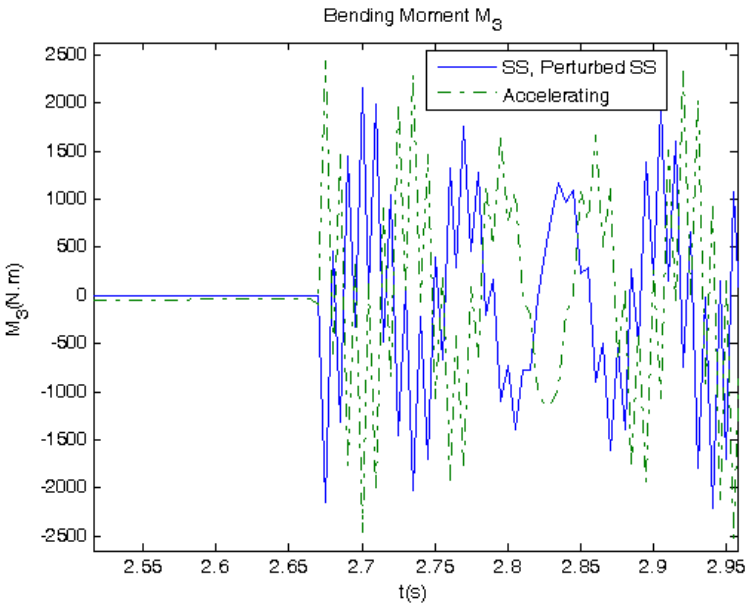

Figure 14. Steady state, accelerating and perturbed bending moment at the root.

therefore be used in order to estimate the degree of sensitivity of each of the output variables to input perturbations.

8. The one-dimensional beam analysis with embedded actuators

For linear piezoelectric materials, the interaction between the electrical and mechanical variables can be described by linear relations. The constitutive equations can be written in matrix form as

$$\{S\} = [s]\{T\} + [d]^t\{E\}, \tag{43}$$

$$\{D\} = [d]\{T\} + [\varepsilon]\{E\}, \tag{44}$$

where S is the strain, D is the electric displacement (charge per unit area), s is the compliance (strain per unit stress), d is the piezoelectric moduli (m/V), and ε is the piezodielectric matrix (F/m). Also, T is the stress vector and E is the electric field intensity (V/m).

With actuators in the structure, the applied force and moment vector per unit length on the structure at every location and every time can be written as the summation of a mechanically applied component and one due to the actuators:

$$\begin{Bmatrix} f \\ m \end{Bmatrix} = \begin{Bmatrix} f_M \\ m_M \end{Bmatrix} + \begin{Bmatrix} f_A \\ m_A \end{Bmatrix}. \tag{45}$$

For a certain actuation scenario, UM/VABS can provide the vector of actuator forces for each active material. Therefore, the whole actuator force is obtained by adding up all of these forces. Substitution

of (45) into (1) gives

$$F' + \tilde{K}F + (f_M + f_A) = \dot{P} + \tilde{\Omega}P \tag{46}$$

$$M' + \tilde{K}M + (\tilde{e}_1 + \tilde{\gamma})F + (m_M + m_A) = \dot{H} + \tilde{\Omega}H + \tilde{V}P. \tag{47}$$

8.1. ***Static active composite airfoil.*** Consider the case of actuation of piezocomposite actuators embedded in a composite wing similar to what is discussed in [Cesnik et al. 2003]. The UM/VABS input file for this case is among the examples provided with the software. The airfoil is a NACA 4415 airfoil with double cells and has a spar located at 38.6% chord from the leading edge, as shown in Figure 15.

Figure 16 illustrates the ply lay-up definitions and orientation angles on the section. A passive 0° ply is used to enclose the cross-section. The inner layers consist of 90°, +45°, −45° and 0° active plies (that is, [0, +90, +45, −45, 0]). The angles are measured with respect to the axis along the wing span. The spar has no active layers.

The material properties of the applied passive and active materials are shown in Table 2. Each layer has a thickness of 3429 μm and a constant electric potential of +1000 V between the two electrodes at a distance of 1100 μm has been applied to the actuators.

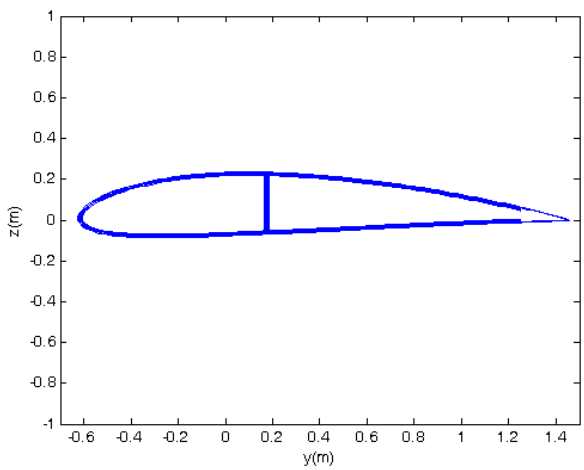

Figure 15. Cross-section of the airfoil.

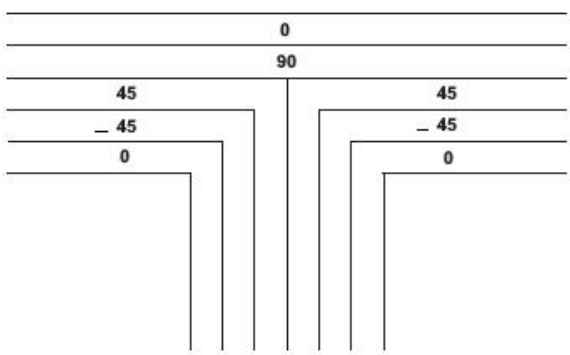

Figure 16. Ply layups and orientation angles of the airfoil cross-section [Cesnik et al. 2003].

	E_{11} GPa	E_{22} GPa	E_{33} GPa	G_{12} GPa	G_{13} GPa	G_{23} GPa	ν_{12}	ν_{13}	ν_{23}	ρ kg/m^3	d_{11} pm/V	d_{12} pm/V	d_{13} pm/V
Passive	19.3	9.8	9.8	5.5	5.5	4.4	0.35	0.35	0.496	1716	—	—	—
Active										4060	310	−130	−130

Table 2. Material properties of active composite airfoil [Cesnik et al. 2003].

Using these data, the stiffness matrix of the cross-section was calculated by UM/VABS as

$$S = \begin{bmatrix} 1.12577\times10^{9} & 3.615437\times10^{3} & -1.28217\times10^{4} & -1.64732\times10^{5} & -2.168324\times10^{5} & -5.681057\times10^{6} \\ 3.615437\times10^{3} & 3.15555\times10^{8} & -4.04582\times10^{5} & -1.0509\times10^{7} & 7.05125\times10^{4} & 4.33983\times10^{3} \\ -1.28217\times10^{4} & -4.04582\times10^{5} & 2.79485\times10^{7} & -1.06215\times10^{7} & 5.81197\times10^{2} & 1.08681\times10^{4} \\ -1.64732\times10^{5} & -1.0509\times10^{7} & -1.06215\times10^{7} & 1.75149\times10^{7} & -2.4470\times10^{3} & 2.00316\times10^{3} \\ -2.168324\times10^{5} & 7.05125\times10^{4} & 5.81197\times10^{2} & -2.4470\times10^{3} & 1.39200\times10^{7} & 1.16753\times10^{5} \\ -5.681057\times10^{6} & 4.33983\times10^{3} & 1.08681\times10^{4} & 2.00316\times10^{3} & 1.16753\times10^{5} & 3.3672\times10^{8} \end{bmatrix} \tag{48}$$

Using UM/VABS, forces, moments, and stress components generated as a result of activating plies at various directions were calculated and some of the results are listed in Table 3. As expected, the active spanwise ply actuation generates the maximum axial force F_1. Also, the $\pm45°$ plies are mainly responsible for twist generation.

Figure 17 illustrates the distribution of various stress components across the cross-section when only the 90° plies are activated by the 1000 V actuation.

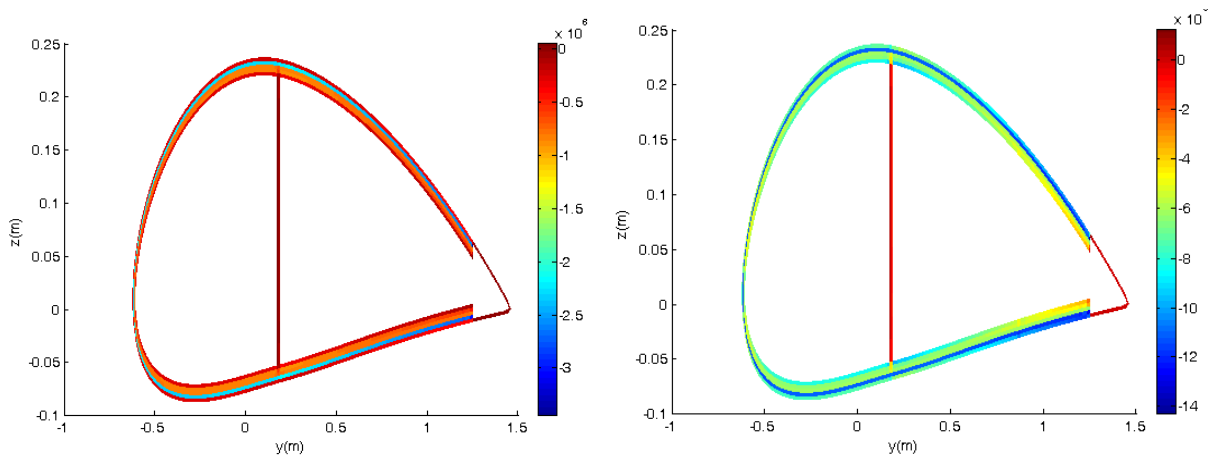

Figure 17. Distribution of the T_{11} (left) and T_{22} (right) stress component due to 1000 V actuation of the 90° plies (distorted image for clarity).

8.2. ***Steady state response of rotating active airfoil.*** Consider the case of actuation of piezocomposite actuators embedded in the composite airfoil discussed before. This time, however, the 3 m beam is rotating at an angular velocity of 100 rad/s and its steady state response under different actuation scenarios is of interest. To this end the method discussed in Section 6 is utilized. Using $\mu = 248.35$ kg/m, the

	0° ply actuation	90° ply actuation	±45° ply actuation	all together
extension (N/m)	71042	−21653	49705	99095
shear F_2 (N/m)	0.603	5.089	2.658	8.349
shear F_3 (N/m)	1.095	19.705	−16.799	4.002
twist (N.m/m)	−0.288	15.67	−238.13	−222.746
bending M_2 (N.m/m)	−41.44	15.19	−33.03	−59.28
bending M_3 (N.m/m)	454.29	−409.01	575.276	620.557

Table 3. Actuation forces and moments generated by active plies at various directions.

UM/VABS two-dimensional analysis resulted in the inertia matrix

$$i = \begin{bmatrix} 77.255 & 0 & 0 \\ 0 & 3.1362 & -0.20052 \\ 0 & -0.20052 & 74.119 \end{bmatrix}. \tag{49}$$

Considering no activation, the steady state response of the beam was obtained. To analyze the effect of coupling, two cases were considered. First, all of the terms in the stiffness and mass matrices were included in the analysis. Then, off-diagonal terms were ignored. The difference of these two solutions provides an overall estimation of the impact of coupling. The results are plotted in Figure 18.

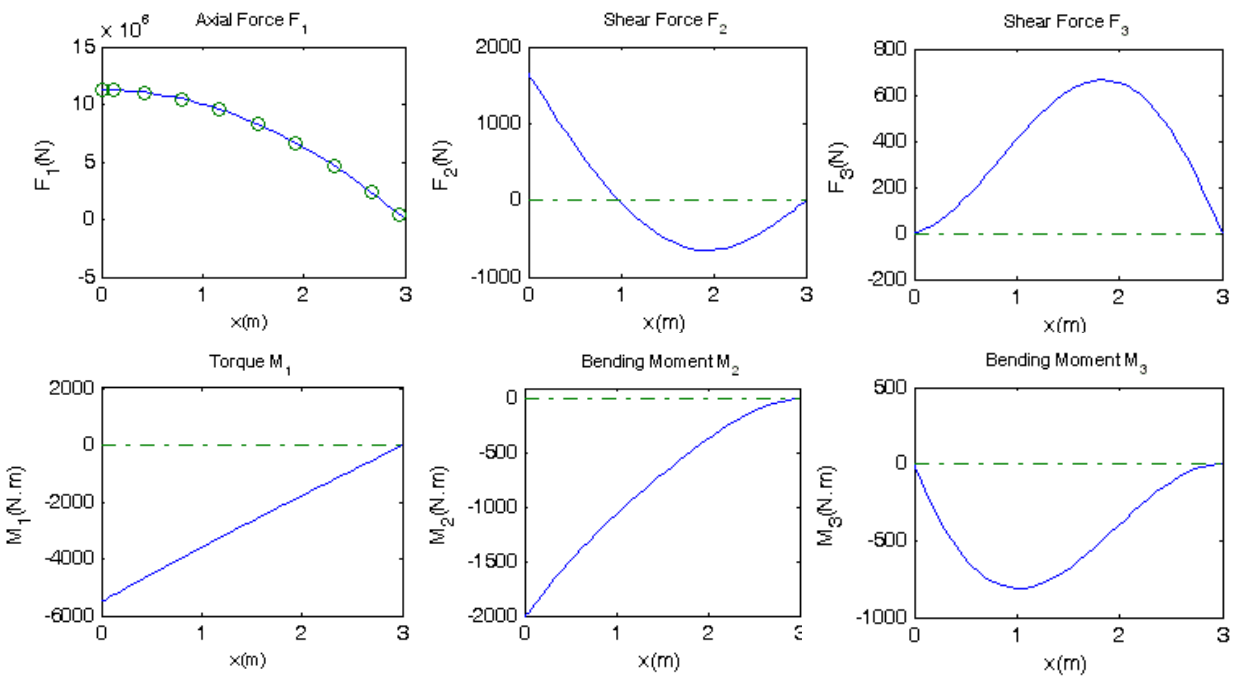

Figure 18. Variation of internal force components (top row) and internal moment components (bottom row) along the beam. The coupled solution is indicated by a solid line, the uncoupled solution by a dashed line or circles.

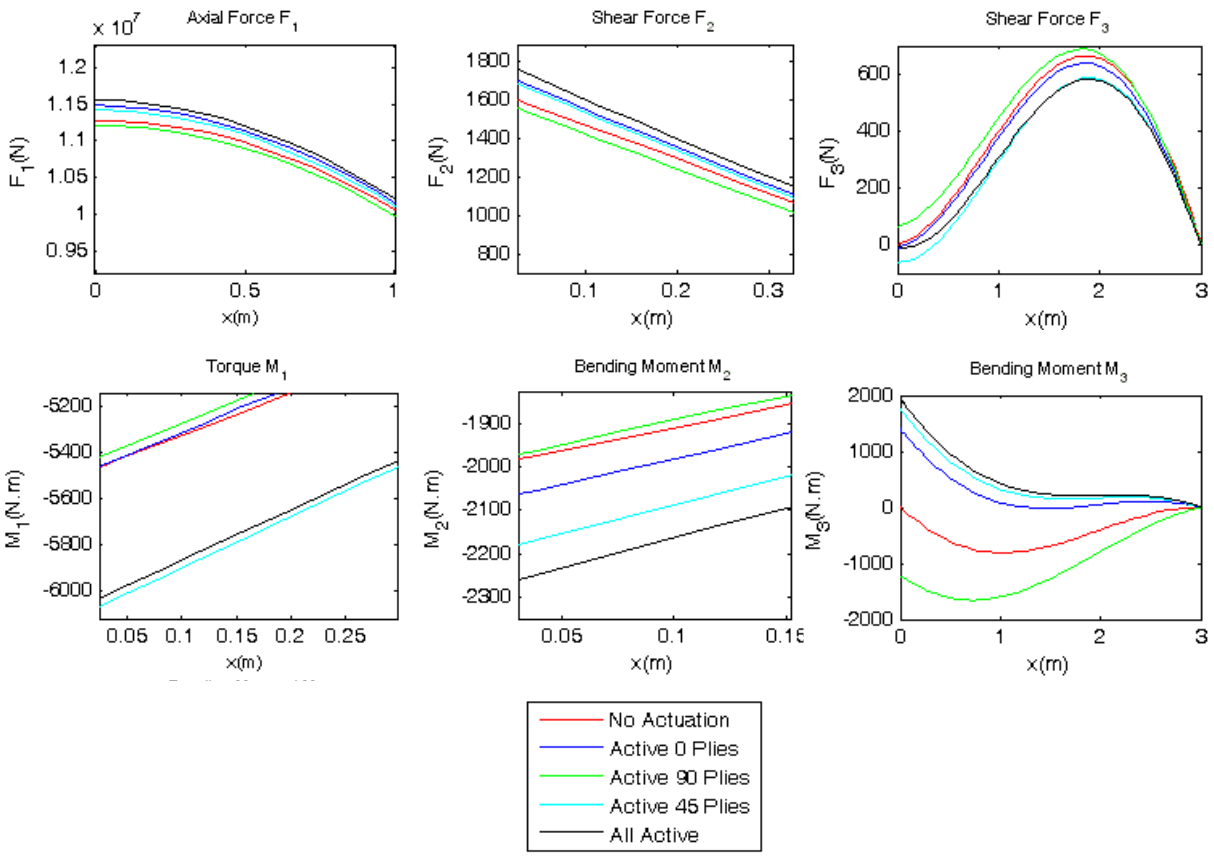

Figure 19. Steady-state variation of internal force components (top row) and internal moment components (bottom row) along the beam, due to various modes of activation of anisotropic piezocomposite actuators (zoomed).

Next, the effect of the activation of each active ply was investigated. To this end, these plies were activated one by one by applying a +1000 V potential to them and the corresponding steady state solutions were obtained. Finally, all of the active plies were activated simultaneously. The results are plotted in Figure 19.

These diagrams can be used for controlling the response of the beam and the load distribution along it. It is observed that the actuators have significant controllability on M_3, but little control on F_1.

9. Conclusions

The structural analysis of geometrically nonlinear passive and active rotating composite beams was presented. The analysis included nonlinear dynamics of accelerating rotating beams and obtaining their transient and steady state responses.

The specific problem considered involved an accelerating rotating beam that starts from rest and at full speed converged to its steady state condition. The steady state behavior was obtained by solving the time-independent form of the governing nonlinear intrinsic differential equations of a beam. The

resulting boundary value problem was solved using the shooting method. The result compared very well with the solution obtained using the FDM.

The next step was the analysis of the effect of input perturbations on the response of rotating beams which are already in their steady state condition. The solution was performed using perturbations and the results were verified against those of the FDM.

Finally, the effect of inclusion of embedded anisotropic piezocomposite actuators in the beam structure was analyzed. In this way, the effect of inclusion of active materials at different orientations on the beam response and on the distributions of stress and stress resultants were illustrated.

Index of notation

A	cross-sectional area of the undeformed beam in x_2-x_3 plane	e_1	$[1\ 0\ 0]^T$
f	applied forces per unit length	F	internal forces
H	sectional angular momenta	g	determinant of metric tensor in curvilinear coordinates
i_2, i_3	cross-sectional mass moment	i_{23}	cross-sectional product of inertia
$\mathcal{K}$	kinetic energy function	$K = k + \bar{\kappa}$	deformed beam curvature vector
k	undeformed beam curvature vector	L	length of the beam
M	internal moments	m	applied moments per unit length
N	number of nodes	P	sectional linear momenta
S	stiffness matrix	t	time
V	velocity field	x_i	global system of coordinates
x_1	axis along the beam	x_2, x_3	cross-sectional axes
$\bar{x}_2$, $\bar{x}_3$	offsets from the reference line of the cross-sectional mass center	γ	$[\gamma_{11}\ 2\gamma_{12}\ 2\gamma_{13}]^T$
		Δ	identity matrix
κ_1	elastic twist	κ_i	elastic bending curvatures, $i = 2, 3$
μ	mass per unit length	ρ	mass density
$\boldsymbol{\Omega}$	angular velocity	$\check{}$	perturbations in space
$\hat{}$	perturbations in time	$'$	x_1-derivative
$\cdot$	time derivative	$\tilde{}$	contraction with last index of $-e_{ijk}$
$\langle\langle u \rangle\rangle$	$\int_A u\sqrt{g}\,dx_2\,dx_3$	$\sqrt{g}$	$1 - x_2k_3 - x_3k_2$

Appendix: Vector J and matrices A, B from Section 4

Recall that a superscript + refers to the next time step. Entries not shown are equal to zero.

$$
\begin{aligned}
J_i(1) = {} & \tfrac{1}{2}(F_{1,i} - F_{1,i+1})/\Delta x + \tfrac{1}{16}(\kappa_{3,i+1}F_{2,i+1} + \kappa_{3,i+1}F_{2,i} + \kappa_{3,i}F_{2,i+1} - 3\kappa_{3,i}F_{2,i}) \\
& - \tfrac{1}{16}(\kappa_{2,i+1}F_{3,i+1} + \kappa_{2,i+1}F_{3,i} + \kappa_{2,i}F_{3,i+1} - 3\kappa_{2,i}F_{3,i}) - \tfrac{1}{4}(f_{1,i+1} + f_{1,i} + f^+_{1,i+1} + f^+_{1,i}) \\
& - \tfrac{1}{2}(P_{1,i} + P_{1,i+1})/\Delta t - \tfrac{1}{16}(\Omega_{3,i+1}P_{2,i+1} + \Omega_{3,i+1}P_{2,i} + \Omega_{3,i}P_{2,i+1} - 3\Omega_{3,i}P_{2,i}) \\
& + \tfrac{1}{16}(\Omega_{2,i+1}P_{3,i+1} + \Omega_{2,i+1}P_{3,i} + \Omega_{2,i}P_{3,i+1} - 3\Omega_{2,i}P_{3,i})
\end{aligned}
$$

$$
\begin{aligned}
J_i(2) &= \tfrac{1}{2}(F_{2,i}-F_{2,i+1})/\Delta x+\tfrac{1}{16}(\kappa_{1,i+1}F_{3,i+1}+\kappa_{1,i+1}F_{3,i}+\kappa_{1,i}F_{3,i+1}-3\kappa_{1,i}F_{3,i})\\
&-\tfrac{1}{16}(\kappa_{3,i+1}F_{1,i+1}+\kappa_{3,i+1}F_{1,i}+\kappa_{3,i}F_{1,i+1}-3\kappa_{3,i}F_{1,i})-\tfrac{1}{4}(f_{2,i+1}+f_{2,i}+f^{+}_{2,i+1}+f^{+}_{2,i})\\
&-\tfrac{1}{2}(P_{2,i}+P_{2,i+1})/\Delta t-\tfrac{1}{16}(\Omega_{1,i+1}P_{3,i+1}+\Omega_{1,i+1}P_{3,i}+\Omega_{1,i}P_{3,i+1}-3\Omega_{1,i}P_{3,i})\\
&+\tfrac{1}{16}(\Omega_{3,i+1}P_{1,i+1}+\Omega_{3,i+1}P_{1,i}+\Omega_{3,i}P_{1,i+1}-3\Omega_{3,i}P_{1,i})
\end{aligned}
$$

$$
\begin{aligned}
J_i(3) &= \tfrac{1}{2}(F_{3,i}-F_{3,i+1})/\Delta x+\tfrac{1}{16}(\kappa_{2,i+1}F_{1,i+1}+\kappa_{2,i+1}F_{1,i}+\kappa_{2,i}F_{1,i+1}-3\kappa_{2,i}F_{1,i})\\
&-\tfrac{1}{16}(\kappa_{1,i+1}F_{2,i+1}+\kappa_{1,i+1}F_{2,i}+\kappa_{1,i}F_{2,i+1}-3\kappa_{1,i}F_{2,i})-\tfrac{1}{4}(f_{3,i+1}+f_{3,i}+f^{+}_{3,i+1}+f^{+}_{3,i})\\
&-\tfrac{1}{2}(P_{3,i}+P_{3,i+1})/\Delta t-\tfrac{1}{16}(\Omega_{2,i+1}P_{1,i+1}+\Omega_{2,i+1}P_{1,i}+\Omega_{2,i}P_{1,i+1}-3\Omega_{2,i}P_{1,i})\\
&+\tfrac{1}{16}(\Omega_{1,i+1}P_{2,i+1}+\Omega_{1,i+1}P_{2,i}+\Omega_{1,i}P_{2,i+1}-3\Omega_{1,i}P_{2,i})
\end{aligned}
$$

$$
\begin{aligned}
J_i(4) &= \tfrac{1}{2}(M_{1,i}-M_{1,i+1})/\Delta x+\tfrac{1}{16}(\kappa_{3,i+1}M_{2,i+1}+\kappa_{3,i+1}M_{2,i}+\kappa_{3,i}M_{2,i+1}-3\kappa_{3,i}M_{2,i})\\
&-\tfrac{1}{16}(\kappa_{2,i+1}M_{3,i+1}+\kappa_{2,i+1}M_{3,i}+\kappa_{2,i}M_{3,i+1}-3\kappa_{2,i}M_{3,i})-\tfrac{1}{4}(m_{1,i+1}+m_{1,i}+m^{+}_{1,i+1}+m^{+}_{1,i})\\
&-\tfrac{1}{2}(H_{1,i}+H_{1,i+1})/\Delta t-\tfrac{1}{16}(\Omega_{3,i+1}H_{2,i+1}+\Omega_{3,i+1}H_{2,i}+\Omega_{3,i}H_{2,i+1}-3\Omega_{3,i}H_{2,i})\\
&+\tfrac{1}{16}(\Omega_{2,i+1}H_{3,i+1}+\Omega_{2,i+1}H_{3,i}+\Omega_{2,i}H_{3,i+1}-3\Omega_{2,i}H_{3,i})\\
&+\tfrac{1}{8}(\gamma_{13,i+1}F_{2,i+1}+\gamma_{13,i+1}F_{2,i}+\gamma_{13,i}F_{2,i+1}-3\gamma_{13,i}F_{2,i})\\
&-\tfrac{1}{8}(\gamma_{12,i+1}F_{3,i+1}+\gamma_{12,i+1}F_{3,i}+\gamma_{12,i}F_{3,i+1}-3\gamma_{12,i}F_{3,i})\\
&-\tfrac{1}{16}(V_{3,i+1}P_{2,i+1}+V_{3,i+1}P_{2,i}+V_{3,i}P_{2,i+1}-3V_{3,i}P_{2,i})+\tfrac{1}{16}(V_{2,i+1}P_{3,i+1}+V_{2,i+1}P_{3,i}+V_{2,i}P_{3,i+1}-3V_{2,i}P_{3,i})
\end{aligned}
$$

$$
\begin{aligned}
J_i(5) &= \tfrac{1}{2}(M_{2,i}-M_{2,i+1})/\Delta x+\tfrac{1}{16}(\kappa_{1,i+1}M_{3,i+1}+\kappa_{1,i+1}M_{3,i}+\kappa_{1,i}M_{3,i+1}-3\kappa_{1,i}M_{3,i})\\
&-\tfrac{1}{16}(\kappa_{3,i+1}M_{1,i+1}+\kappa_{3,i+1}M_{1,i}+\kappa_{3,i}M_{1,i+1}-3\kappa_{3,i}M_{1,i})-\tfrac{1}{4}(m_{2,i+1}+m_{2,i}+m^{+}_{2,i+1}+m^{+}_{2,i})\\
&-\tfrac{1}{2}(H_{2,i}+H_{2,i+1})/\Delta t-\tfrac{1}{16}(\Omega_{1,i+1}H_{3,i+1}+\Omega_{1,i+1}H_{3,i}+\Omega_{1,i}H_{3,i+1}-3\Omega_{1,i}H_{3,i})\\
&+\tfrac{1}{16}(\Omega_{3,i+1}H_{1,i+1}+\Omega_{3,i+1}H_{1,i}+\Omega_{3,i}H_{1,i+1}-3\Omega_{3,i}H_{1,i})+\tfrac{1}{4}(F_{3,i}+F_{3,i+1})\\
&+\tfrac{1}{16}(\gamma_{11,i+1}F_{3,i+1}+\gamma_{11,i+1}F_{3,i}+\gamma_{11,i}F_{3,i+1}-3\gamma_{11,i}F_{3,i})\\
&-\tfrac{1}{8}(\gamma_{13,i+1}F_{1,i+1}+\gamma_{13,i+1}F_{1,i}+\gamma_{13,i}F_{1,i+1}-3\gamma_{13,i}F_{1,i})\\
&-\tfrac{1}{16}(V_{1,i+1}P_{3,i+1}+V_{1,i+1}P_{3,i}+V_{1,i}P_{3,i+1}-3V_{1,i}P_{3,i})+\tfrac{1}{16}(V_{3,i+1}P_{1,i+1}+V_{3,i+1}P_{1,i}+V_{3,i}P_{1,i+1}-3V_{3,i}P_{1,i})
\end{aligned}
$$

$$
\begin{aligned}
J_i(6) &= \tfrac{1}{2}(M_{3,i}-M_{3,i+1})/\Delta x+\tfrac{1}{16}(\kappa_{2,i+1}M_{1,i+1}+\kappa_{2,i+1}M_{1,i}+\kappa_{2,i}M_{1,i+1}-3\kappa_{2,i}M_{1,i})\\
&-\tfrac{1}{16}(\kappa_{1,i+1}M_{2,i+1}+\kappa_{1,i+1}M_{2,i}+\kappa_{1,i}M_{2,i+1}-3\kappa_{1,i}M_{2,i})-\tfrac{1}{4}(m_{3,i+1}+m_{3,i}+m^{+}_{3,i+1}+m^{+}_{3,i})\\
&-\tfrac{1}{2}(H_{3,i}+H_{3,i+1})/\Delta t-\tfrac{1}{16}(\Omega_{2,i+1}H_{1,i+1}+\Omega_{2,i+1}H_{1,i}+\Omega_{2,i}H_{1,i+1}-3\Omega_{2,i}H_{1,i})\\
&+\tfrac{1}{16}(\Omega_{1,i+1}H_{2,i+1}+\Omega_{1,i+1}H_{2,i}+\Omega_{1,i}H_{2,i+1}-3\Omega_{1,i}H_{2,i})-\tfrac{1}{4}(F_{2,i}+F_{2,i+1})\\
&+\tfrac{1}{16}(\gamma_{11,i+1}F_{2,i+1}+\gamma_{11,i+1}F_{2,i}+\gamma_{11,i}F_{2,i+1}-3\gamma_{11,i}F_{2,i})\\
&+\tfrac{1}{8}(\gamma_{12,i+1}F_{1,i+1}+\gamma_{12,i+1}F_{1,i}+\gamma_{12,i}F_{1,i+1}-3\gamma_{12,i}F_{1,i})\\
&-\tfrac{1}{16}(V_{2,i+1}P_{1,i+1}+V_{2,i+1}P_{1,i}+V_{2,i}P_{1,i+1}-3V_{2,i}P_{1,i})+\tfrac{1}{16}(V_{1,i+1}P_{2,i+1}+V_{1,i+1}P_{2,i}+V_{1,i}P_{2,i+1}-3V_{1,i}P_{2,i})
\end{aligned}
$$

$$
\begin{aligned}
J_i(7) &= \tfrac{1}{2}(V_{1,i}-V_{1,i+1})/\Delta x+\tfrac{1}{16}(\kappa_{3,i+1}V_{2,i+1}+\kappa_{3,i+1}V_{2,i}+\kappa_{3,i}V_{2,i+1}-3\kappa_{3,i}V_{2,i})\\
&-\tfrac{1}{16}(\kappa_{2,i+1}V_{3,i+1}+\kappa_{2,i+1}V_{3,i}+\kappa_{2,i}V_{3,i+1}-3\kappa_{2,i}V_{3,i})\\
&+\tfrac{1}{8}(\gamma_{13,i+1}\Omega_{2,i+1}+\gamma_{13,i+1}\Omega_{2,i}+\gamma_{13,i}\Omega_{2,i+1}-3\gamma_{13,i}\Omega_{2,i})\\
&-\tfrac{1}{8}(\gamma_{12,i+1}\Omega_{3,i+1}+\gamma_{12,i+1}\Omega_{3,i}+\gamma_{12,i}\Omega_{3,i+1}-3\gamma_{12,i}\Omega_{3,i})-\tfrac{1}{2}(\gamma_{11,i}+\gamma_{11,i+1})/\Delta t
\end{aligned}
$$

$$J_i(8) = \tfrac{1}{2}(V_{2,i} - V_{2,i+1})/\Delta x + \tfrac{1}{16}(\kappa_{1,i+1}V_{3,i+1} + \kappa_{1,i+1}V_{3,i} + \kappa_{1,i}V_{3,i+1} - 3\kappa_{1,i}V_{3,i})$$
$$- \tfrac{1}{16}(\kappa_{3,i+1}V_{1,i+1} + \kappa_{3,i+1}V_{1,i} + \kappa_{3,i}V_{1,i+1} - 3\kappa_{3,i}V_{1,i}) + \tfrac{1}{4}(\Omega_{3,i} + \Omega_{3,i+1})$$
$$+ \tfrac{1}{16}(\gamma_{11,i+1}\Omega_{3,i+1} + \gamma_{11,i+1}\Omega_{3,i} + \gamma_{11,i}\Omega_{3,i+1} - 3\gamma_{11,i}\Omega_{3,i})$$
$$- \tfrac{1}{8}(\gamma_{13,i+1}\Omega_{1,i+1} + \gamma_{13,i+1}\Omega_{1,i} + \gamma_{13,i}\Omega_{1,i+1} - 3\gamma_{13,i}\Omega_{1,i}) - (\gamma_{12,i} + \gamma_{12,i+1})/\Delta t$$

$$J_i(9) = \tfrac{1}{2}(V_{3,i} - V_{3,i+1})/\Delta x + \tfrac{1}{16}(\kappa_{2,i+1}V_{1,i+1} + \kappa_{2,i+1}V_{1,i} + \kappa_{2,i}V_{1,i+1} - 3\kappa_{2,i}V_{1,i})$$
$$- \tfrac{1}{16}(\kappa_{1,i+1}V_{2,i+1} + \kappa_{1,i+1}V_{2,i} + \kappa_{1,i}V_{2,i+1} - 3\kappa_{1,i}V_{2,i}) - \tfrac{1}{4}(\Omega_{2,i} + \Omega_{2,i+1})$$
$$- \tfrac{1}{16}(\gamma_{11,i+1}\Omega_{2,i+1} + \gamma_{11,i+1}\Omega_{2,i} + \gamma_{11,i}\Omega_{2,i+1} - 3\gamma_{11,i}\Omega_{2,i})$$
$$+ \tfrac{1}{8}(\gamma_{12,i+1}\Omega_{1,i+1} + \gamma_{12,i+1}\Omega_{1,i} + \gamma_{12,i}\Omega_{1,i+1} - 3\gamma_{12,i}\Omega_{1,i}) - (\gamma_{13,i} + \gamma_{13,i+1})/\Delta t$$

$$J_i(10) = \tfrac{1}{2}(\Omega_{1,i} - \Omega_{1,i+1})/\Delta x + \tfrac{1}{16}(\kappa_{3,i+1}\Omega_{2,i+1} + \kappa_{3,i+1}\Omega_{2,i} + \kappa_{3,i}\Omega_{2,i+1} - 3\kappa_{3,i}\Omega_{2,i})$$
$$- \tfrac{1}{16}(\kappa_{2,i+1}\Omega_{3,i+1} + \kappa_{2,i+1}\Omega_{3,i} + \kappa_{2,i}\Omega_{3,i+1} - 3\kappa_{2,i}\Omega_{3,i}) - \tfrac{1}{2}(\kappa_{1,i} + \kappa_{1,i+1})/\Delta t$$

$$J_i(11) = \tfrac{1}{2}(\Omega_{2,i} - \Omega_{2,i+1})/\Delta x + \tfrac{1}{16}(\kappa_{1,i+1}\Omega_{3,i+1} + \kappa_{1,i+1}\Omega_{3,i} + \kappa_{1,i}\Omega_{3,i+1} - 3\kappa_{1,i}\Omega_{3,i})$$
$$- \tfrac{1}{16}(\kappa_{3,i+1}\Omega_{1,i+1} + \kappa_{3,i+1}\Omega_{1,i} + \kappa_{3,i}\Omega_{1,i+1} - 3\kappa_{3,i}\Omega_{1,i}) - \tfrac{1}{2}(\kappa_{2,i} + \kappa_{2,i+1})/\Delta t$$

$$J_i(12) = \tfrac{1}{2}(\Omega_{3,i} - \Omega_{3,i+1})/\Delta x + \tfrac{1}{16}(\kappa_{2,i+1}\Omega_{1,i+1} + \kappa_{2,i+1}\Omega_{1,i} + \kappa_{2,i}\Omega_{1,i+1} - 3\kappa_{2,i}\Omega_{1,i})$$
$$- \tfrac{1}{16}(\kappa_{1,i+1}\Omega_{2,i+1} + \kappa_{1,i+1}\Omega_{2,i} + \kappa_{1,i}\Omega_{2,i+1} - 3\kappa_{1,i}\Omega_{2,i}) - \tfrac{1}{2}(\kappa_{3,i} + \kappa_{3,i+1})/\Delta t$$

$$J_i(13) = -\tfrac{1}{4}(P_{1,i} + P_{1,i+1}) + \tfrac{1}{4}\mu(V_{1,i} + V_{1,i+1}) + \tfrac{1}{4}\mu\bar{x}_3(\Omega_{2,i} + \Omega_{2,i+1}) - \tfrac{1}{4}\mu\bar{x}_2(\Omega_{3,i} + \Omega_{3,i+1})$$

$$J_i(14) = -\tfrac{1}{4}(P_{2,i} + P_{2,i+1}) + \tfrac{1}{4}\mu(V_{2,i} + V_{2,i+1}) - \tfrac{1}{4}\mu\bar{x}_3(\Omega_{1,i} + \Omega_{1,i+1})$$

$$J_i(15) = -\tfrac{1}{4}(P_{3,i} + P_{3,i+1}) + \tfrac{1}{4}\mu(V_{3,i} + V_{3,i+1}) + \tfrac{1}{4}\mu\bar{x}_2(\Omega_{1,i} + \Omega_{1,i+1})$$

$$J_i(16) = -\tfrac{1}{4}(H_{1,i} + H_{1,i+1}) - \tfrac{1}{4}\mu\bar{x}_3(V_{2,i} + V_{2,i+1}) + \tfrac{1}{4}\mu\bar{x}_2(V_{3,i} + V_{3,i+1})$$
$$+ \tfrac{1}{4}i(1,1)(\Omega_{1,i} + \Omega_{1,i+1}) + \tfrac{1}{4}i(1,2)(\Omega_{2,i} + \Omega_{2,i+1}) + \tfrac{1}{4}i(1,3)(\Omega_{3,i} + \Omega_{3,i+1})$$

$$J_i(17) = -\tfrac{1}{4}(H_{2,i} + H_{2,i+1}) + \tfrac{1}{4}\mu\bar{x}_3(V_{1,i} + V_{1,i+1}) + \tfrac{1}{4}i(2,1)(\Omega_{1,i} + \Omega_{1,i+1})$$
$$+ \tfrac{1}{4}i(2,2)(\Omega_{2,i} + \Omega_{2,i+1}) + \tfrac{1}{4}i(2,3)(\Omega_{3,i} + \Omega_{3,i+1})$$

$$J_i(18) = -\tfrac{1}{4}(H_{3,i} + H_{3,i+1}) - \tfrac{1}{4}\mu\bar{x}_2(V_{1,i} + V_{1,i+1}) + \tfrac{1}{4}i(3,1)(\Omega_{1,i} + \Omega_{1,i+1})$$
$$+ \tfrac{1}{4}i(3,2)(\Omega_{2,i} + \Omega_{2,i+1}) + \tfrac{1}{4}i(3,3)(\Omega_{3,i} + \Omega_{3,i+1})$$

$$J_i(19) = -\tfrac{1}{4}(\gamma_{11,i} + \gamma_{11,i+1}) + \tfrac{1}{4}R(1,1)(F_{1,i} + F_{1,i+1})$$
$$+ \tfrac{1}{4}R(1,2)(F_{2,i} + F_{2,i+1}) + \tfrac{1}{4}R(1,3)(F_{3,i} + F_{3,i+1}) + \tfrac{1}{4}Z(1,1)(M_{1,i} + M_{1,i+1})$$
$$+ \tfrac{1}{4}Z(1,2)(M_{2,i} + M_{2,i+1}) + \tfrac{1}{4}Z(1,3)(M_{3,i} + M_{3,i+1})$$

$$J_i(20) = -\tfrac{1}{2}(\gamma_{12,i} + \gamma_{12,i+1}) + \tfrac{1}{4}R(2,1)(F_{1,i} + F_{1,i+1})$$
$$+ \tfrac{1}{4}R(2,2)(F_{2,i} + F_{2,i+1}) + \tfrac{1}{4}R(2,3)(F_{3,i} + F_{3,i+1}) + \tfrac{1}{4}Z(2,1)(M_{1,i} + M_{1,i+1})$$
$$+ \tfrac{1}{4}Z(2,2)(M_{2,i} + M_{2,i+1}) + \tfrac{1}{4}Z(2,3)(M_{3,i} + M_{3,i+1})$$

$$J_i(21) = -\tfrac{1}{2}(\gamma_{13,i} + \gamma_{13,i+1}) + \tfrac{1}{4}R(3,1)(F_{1,i} + F_{1,i+1})$$
$$+ \tfrac{1}{4}R(3,2)(F_{2,i} + F_{2,i+1}) + \tfrac{1}{4}R(3,3)(F_{3,i} + F_{3,i+1}) + \tfrac{1}{4}Z(3,1)(M_{1,i} + M_{1,i+1})$$
$$+ \tfrac{1}{4}Z(3,2)(M_{2,i} + M_{2,i+1}) + \tfrac{1}{4}Z(3,3)(M_{3,i} + M_{3,i+1})$$

$$J_i(22) = -\tfrac{1}{4}(\kappa_{1,i}+\kappa_{1,i+1})+\tfrac{1}{4}Z(1,1)(F_{1,i}+F_{1,i+1})$$
$$+\tfrac{1}{4}Z(2,1)(F_{2,i}+F_{2,i+1})+\tfrac{1}{4}Z(3,1)(F_{3,i}+F_{3,i+1})+\tfrac{1}{4}T(1,1)(M_{1,i}+M_{1,i+1})$$
$$+\tfrac{1}{4}T(1,2)(M_{2,i}+M_{2,i+1})+\tfrac{1}{4}T(1,3)(M_{3,i}+M_{3,i+1})$$

$$J_i(23) = -\tfrac{1}{4}(\kappa_{2,i}+\kappa_{2,i+1})+\tfrac{1}{4}Z(1,2)(F_{1,i}+F_{1,i+1})$$
$$+\tfrac{1}{4}Z(2,2)(F_{2,i}+F_{2,i+1})+\tfrac{1}{4}Z(3,2)(F_{3,i}+F_{3,i+1})+\tfrac{1}{4}T(2,1)(M_{1,i}+M_{1,i+1})$$
$$+\tfrac{1}{4}T(2,2)(M_{2,i}+M_{2,i+1})+\tfrac{1}{4}T(2,3)(M_{3,i}+M_{3,i+1})$$

$$J_i(24) = -\tfrac{1}{4}(\kappa_{3,i}+\kappa_{3,i+1})+\tfrac{1}{4}Z(1,3)(F_{1,i}+F_{1,i+1})+\tfrac{1}{4}Z(2,3)(F_{2,i}+F_{2,i+1})$$
$$+\tfrac{1}{4}Z(3,3)(F_{3,i}+F_{3,i+1})+\tfrac{1}{4}T(3,1)(M_{1,i}+M_{1,i+1})$$
$$+\tfrac{1}{4}T(3,2)(M_{2,i}+M_{2,i+1})+\tfrac{1}{4}T(3,3)(M_{3,i}+M_{3,i+1})$$

A_i ($-$ sign) or B_i ($+$ sign) columns 1:3 rows 1:6

$$\begin{bmatrix} \pm 1/(2\Delta x) & -\frac{1}{16}(\kappa_{3,i+1}+3\kappa_{3,i}) & \frac{1}{16}(\kappa_{2,i+1}+3\kappa_{2,i}) \\ \frac{1}{16}(\kappa_{3,i+1}+3\kappa_{3,i}) & \pm 1/(2\Delta x) & -\frac{1}{16}(\kappa_{1,i+1}+3\kappa_{1,i}) \\ -\frac{1}{16}(\kappa_{2,i+1}+3\kappa_{2,i}) & \frac{1}{16}(\kappa_{1,i+1}+3\kappa_{1,i}) & \pm 1/(2\Delta x) \\ 0 & -\frac{1}{8}(\gamma_{13,i+1}+3\gamma_{13,i}) & \frac{1}{8}(\gamma_{12,i+1}+3\gamma_{12,i}) \\ \frac{1}{8}(\gamma_{13,i+1}+3\gamma_{13,i}) & 0 & -\frac{1}{4}-\frac{1}{16}(\gamma_{11,i+1}+3\gamma_{11,i}) \\ -\frac{1}{8}(\gamma_{12,i+1}+3\gamma_{12,i}) & \frac{1}{4}+\frac{1}{16}(\gamma_{11,i+1}+3\gamma_{11,i}) & 0 \end{bmatrix}$$

A_i or B_i columns 1:3 rows 19:24

$$\begin{bmatrix} -\frac{1}{4}R(1,1) & -\frac{1}{4}R(1,2) & -\frac{1}{4}R(1,3) \\ -\frac{1}{4}R(2,1) & -\frac{1}{4}R(2,2) & -\frac{1}{4}R(2,3) \\ -\frac{1}{4}R(3,1) & -\frac{1}{4}R(3,2) & -\frac{1}{4}R(3,3) \\ -\frac{1}{4}Z(1,1) & -\frac{1}{4}Z(2,1) & -\frac{1}{4}Z(3,1) \\ -\frac{1}{4}Z(1,2) & -\frac{1}{4}Z(2,2) & -\frac{1}{4}Z(3,2) \\ -\frac{1}{4}Z(1,3) & -\frac{1}{4}Z(2,3) & -\frac{1}{4}Z(3,3) \end{bmatrix}$$

A_i ($-$ sign) or B_i ($+$ sign) columns 4:6 rows 4:6

$$\begin{bmatrix} \pm 1/(2\Delta x) & -\frac{1}{16}(\kappa_{3,i+1}+3\kappa_{3,i}) & \frac{1}{16}(\kappa_{2,i+1}+3\kappa_{2,i}) \\ \frac{1}{16}(\kappa_{3,i+1}+3\kappa_{3,i}) & \pm 1/(2\Delta x) & -\frac{1}{16}(\kappa_{1,i+1}+3\kappa_{1,i}) \\ -\frac{1}{16}(\kappa_{2,i+1}+3\kappa_{2,i}) & \frac{1}{16}(\kappa_{1,i+1}+3\kappa_{1,i}) & \pm 1/(2\Delta x) \end{bmatrix}$$

A_i or B_i columns 4:6 rows 19:24

$$\begin{bmatrix} -\frac{1}{4}Z(1,1) & -\frac{1}{4}Z(1,2) & -\frac{1}{4}Z(1,3) \\ -\frac{1}{4}Z(2,1) & -\frac{1}{4}Z(2,2) & -\frac{1}{4}Z(2,3) \\ -\frac{1}{4}Z(3,1) & -\frac{1}{4}Z(3,2) & -\frac{1}{4}Z(3,3) \\ -\frac{1}{4}T(1,1) & -\frac{1}{4}T(1,2) & -\frac{1}{4}T(1,3) \\ -\frac{1}{4}T(2,1) & -\frac{1}{4}T(2,2) & -\frac{1}{4}T(2,3) \\ -\frac{1}{4}T(3,1) & -\frac{1}{4}T(3,2) & -\frac{1}{4}T(3,3) \end{bmatrix}$$

A_i ($-$ sign) or B_i ($+$ sign) columns 7:9 rows 4:9

$$\begin{bmatrix} 0 & -\frac{1}{16}(P_{3,i+1}+3P_{3,i}) & \frac{1}{16}(P_{2,i+1}+3P_{2,i}) \\ \frac{1}{16}(P_{3,i+1}+3P_{3,i}) & 0 & -\frac{1}{16}(P_{1,i+1}+3P_{1,i}) \\ -\frac{1}{16}(P_{2,i+1}+3P_{2,i}) & \frac{1}{16}(P_{1,i+1}+3P_{1,i}) & 0 \\ \pm 1/(2\Delta x) & -\frac{1}{16}(\kappa_{3,i+1}+3\kappa_{3,i}) & \frac{1}{16}(\kappa_{2,i+1}+3\kappa_{2,i}) \\ \frac{1}{16}(\kappa_{3,i+1}+3\kappa_{3,i}) & \pm 1/(2\Delta x) & -\frac{1}{16}(\kappa_{1,i+1}+3\kappa_{1,i}) \\ -\frac{1}{16}(\kappa_{2,i+1}+3\kappa_{2,i}) & \frac{1}{16}(\kappa_{1,i+1}+3\kappa_{1,i}) & \pm 1/(2\Delta x) \end{bmatrix}$$

A_i or B_i columns 7:9 rows 13:18

$$\begin{bmatrix} -\frac{1}{4}\mu & 0 & 0 \\ 0 & -\frac{1}{4}\mu & 0 \\ 0 & 0 & -\frac{1}{4}\mu \\ 0 & \frac{1}{4}\mu\bar{x}_3 & -\frac{1}{4}\mu\bar{x}_2 \\ -\frac{1}{4}\mu\bar{x}_3 & 0 & 0 \\ \frac{1}{4}\mu\bar{x}_2 & 0 & 0 \end{bmatrix}$$

A_i or B_i columns 10:12 rows 1:6

$$\begin{bmatrix} 0 & -\frac{1}{16}(P_{3,i+1}+3P_{3,i}) & \frac{1}{16}(P_{2,i+1}+3P_{2,i}) \\ \frac{1}{16}(P_{3,i+1}+3P_{3,i}) & 0 & -\frac{1}{16}(P_{1,i+1}+3P_{1,i}) \\ -\frac{1}{16}(P_{2,i+1}+3P_{2,i}) & \frac{1}{16}(P_{1,i+1}+3P_{1,i}) & 0 \\ 0 & -\frac{1}{16}(H_{3,i+1}+3H_{3,i}) & \frac{1}{16}(H_{2,i+1}+3H_{2,i}) \\ \frac{1}{16}(H_{3,i+1}+3H_{3,i}) & 0 & -\frac{1}{16}(H_{1,i+1}+3H_{1,i}) \\ -\frac{1}{16}(H_{2,i+1}+3H_{2,i}) & \frac{1}{16}(H_{1,i+1}+3H_{1,i}) & 0 \end{bmatrix}$$

A_i (− sign) or B_i (+ sign) columns 10:12 rows 7:12

$$\begin{bmatrix} 0 & -\frac{1}{8}(\gamma_{13,i+1}+3\gamma_{13,i}) & \frac{1}{8}(\gamma_{12,i+1}+3\gamma_{12,i}) \\ \frac{1}{8}(\gamma_{13,i+1}+3\gamma_{13,i}) & 0 & -\frac{1}{4}-\frac{1}{16}(\gamma_{11,i+1}+3\gamma_{11,i}) \\ -\frac{1}{8}(\gamma_{12,i+1}+3\gamma_{12,i}) & \frac{1}{4}+\frac{1}{16}(\gamma_{11,i+1}+3\gamma_{11,i}) & 0 \\ \pm 1/(2\Delta x) & -\frac{1}{16}(\kappa_{3,i+1}+3\kappa_{3,i}) & \frac{1}{16}(\kappa_{2,i+1}+3\kappa_{2,i}) \\ \frac{1}{16}(\kappa_{3,i+1}+3\kappa_{3,i}) & \pm 1/(2\Delta x) & -\frac{1}{16}(\kappa_{1,i+1}+3\kappa_{1,i}) \\ -\frac{1}{16}(\kappa_{2,i+1}+3\kappa_{2,i}) & \frac{1}{16}(\kappa_{1,i+1}+3\kappa_{1,i}) & \pm 1/(2\Delta x) \end{bmatrix}$$

A_i or B_i columns 10:12 rows 13:18

$$\begin{bmatrix} 0 & -\frac{1}{4}\mu\bar{x}_3 & \frac{1}{4}\mu\bar{x}_2 \\ \frac{1}{4}\mu\bar{x}_3 & 0 & 0 \\ -\frac{1}{4}\mu\bar{x}_2 & 0 & 0 \\ -\frac{1}{4}i(1,1) & -\frac{1}{4}i(1,2) & -\frac{1}{4}i(1,3) \\ -\frac{1}{4}i(2,1) & -\frac{1}{4}i(2,2) & -\frac{1}{4}i(2,3) \\ -\frac{1}{4}i(3,1) & -\frac{1}{4}i(3,2) & -\frac{1}{4}i(3,3) \end{bmatrix}$$

A_i or B_i columns 13:15 rows 1:6

$$\begin{bmatrix} -1/(2\Delta t) & \frac{1}{16}(\Omega_{3,i+1}+3\Omega_{3,i}) & -\frac{1}{16}(\Omega_{2,i+1}+3\Omega_{2,i}) \\ -\frac{1}{16}(\Omega_{3,i+1}+3\Omega_{3,i}) & -1/(2\Delta t) & \frac{1}{16}(\Omega_{1,i+1}+3\Omega_{1,i}) \\ \frac{1}{16}(\Omega_{2,i+1}+3\Omega_{2,i}) & -\frac{1}{16}(\Omega_{1,i+1}+3\Omega_{1,i}) & -1/(2\Delta t) \\ 0 & \frac{1}{16}(V_{3,i+1}+3V_{3,i}) & -\frac{1}{16}(V_{2,i+1}+3V_{2,i}) \\ -\frac{1}{16}(V_{3,i+1}+3V_{3,i}) & 0 & \frac{1}{16}(V_{1,i+1}+3V_{1,i}) \\ \frac{1}{16}(V_{2,i+1}+3V_{2,i}) & -\frac{1}{16}(V_{1,i+1}+3V_{1,i}) & 0 \end{bmatrix}$$

A_i or B_i columns 13:15 rows 13:15

$$\begin{bmatrix} \frac{1}{4} & 0 & 0 \\ 0 & \frac{1}{4} & 0 \\ 0 & 0 & \frac{1}{4} \end{bmatrix}$$

A_i or B_i columns 16:18 rows 4:6

$$\begin{bmatrix} -1/(2\Delta t) & \frac{1}{16}(\Omega_{3,i+1}+3\Omega_{3,i}) & -\frac{1}{16}(\Omega_{2,i+1}+3\Omega_{2,i}) \\ -\frac{1}{16}(\Omega_{3,i+1}+3\Omega_{3,i}) & -1/(2\Delta t) & \frac{1}{16}(\Omega_{1,i+1}+3\Omega_{1,i}) \\ \frac{1}{16}(\Omega_{2,i+1}+3\Omega_{2,i}) & -\frac{1}{16}(\Omega_{1,i+1}+3\Omega_{1,i}) & -1/(2\Delta t) \end{bmatrix}$$

A_i or B_i columns 16:18 rows 16:18

$$\begin{bmatrix} \frac{1}{4} & 0 & 0 \\ 0 & \frac{1}{4} & 0 \\ 0 & 0 & \frac{1}{4} \end{bmatrix}$$

A_i or B_i columns 19:21 rows 4:9

$$\begin{bmatrix} 0 & \frac{1}{16}(F_{3,i+1}+3F_{3,i}) & -\frac{1}{16}(F_{2,i+1}+3F_{2,i}) \\ -\frac{1}{16}(F_{3,i+1}+3F_{3,i}) & 0 & \frac{1}{16}(F_{1,i+1}+3F_{1,i}) \\ \frac{1}{16}(F_{2,i+1}+3F_{2,i}) & -\frac{1}{16}(F_{1,i+1}+3F_{1,i}) & 0 \\ -1/(2\Delta t) & \frac{1}{16}(\Omega_{3,i+1}+3\Omega_{3,i}) & -\frac{1}{16}(\Omega_{2,i+1}+3\Omega_{2,i}) \\ -\frac{1}{16}(\Omega_{3,i+1}+3\Omega_{3,i}) & -1/(2\Delta t) & \frac{1}{16}(\Omega_{1,i+1}+3\Omega_{1,i}) \\ \frac{1}{16}(\Omega_{2,i+1}+3\Omega_{2,i}) & -\frac{1}{16}(\Omega_{1,i+1}+3\Omega_{1,i}) & -1/(2\Delta t) \end{bmatrix}$$

A_i or B_i columns 19:21 rows 19:21

$$\begin{bmatrix} \frac{1}{4} & 0 & 0 \\ 0 & \frac{1}{4} & 0 \\ 0 & 0 & \frac{1}{4} \end{bmatrix}$$

A_i or B_i columns 22:24 rows 1:6

$$\begin{bmatrix} 0 & \frac{1}{16}(F_{3,i+1}+3F_{3,i}) & -\frac{1}{16}(F_{2,i+1}+3F_{2,i}) \\ -\frac{1}{16}(F_{3,i+1}+3F_{3,i}) & 0 & \frac{1}{16}(F_{1,i+1}+3F_{1,i}) \\ \frac{1}{16}(F_{2,i+1}+3F_{2,i}) & -\frac{1}{16}(F_{1,i+1}+3F_{1,i}) & 0 \\ 0 & \frac{1}{16}(M_{3,i+1}+3M_{3,i}) & -\frac{1}{16}(M_{2,i+1}+3M_{2,i}) \\ -\frac{1}{16}(M_{3,i+1}+3M_{3,i}) & 0 & \frac{1}{16}(M_{1,i+1}+3M_{1,i}) \\ \frac{1}{16}(M_{2,i+1}+3M_{2,i}) & -\frac{1}{16}(M_{1,i+1}+3M_{1,i}) & 0 \end{bmatrix}$$

A_i or B_i columns 22:24 rows 7:12

$$\begin{bmatrix} 0 & \frac{1}{16}(V_{3,i+1}+3V_{3,i}) & -\frac{1}{16}(V_{2,i+1}+3V_{2,i}) \\ -\frac{1}{16}(V_{3,i+1}+3V_{3,i}) & 0 & \frac{1}{16}(V_{1,i+1}+3V_{1,i}) \\ \frac{1}{16}(V_{2,i+1}+3V_{2,i}) & -\frac{1}{16}(V_{1,i+1}+3V_{1,i}) & 0 \\ -1/(2\Delta t) & \frac{1}{16}(\Omega_{3,i+1}+3\Omega_{3,i}) & -\frac{1}{16}(\Omega_{2,i+1}+3\Omega_{2,i}) \\ -\frac{1}{16}(\Omega_{3,i+1}+3\Omega_{3,i}) & -1/(2\Delta t) & \frac{1}{16}(\Omega_{1,i+1}+3\Omega_{1,i}) \\ \frac{1}{16}(\Omega_{2,i+1}+3\Omega_{2,i}) & -\frac{1}{16}(\Omega_{1,i+1}+3\Omega_{1,i}) & -1/(2\Delta t) \end{bmatrix}$$

A_i or B_i columns 22:24 rows 22:24

$$\begin{bmatrix} \frac{1}{4} & 0 & 0 \\ 0 & \frac{1}{4} & 0 \\ 0 & 0 & \frac{1}{4} \end{bmatrix}$$

References

[Berdichevskii 1981] V. L. Berdichevskii, "On the energy of an elastic rod", *Prikl. Mat. Mekh.* **45**:4 (1981), 704–718. In Russian: translation in *J. Appl. Math. Mech.* **45**:4, (1981), 518–529.

[Cesnik and Palacios 2003] C. E. S. Cesnik and R. Palacios, "Modeling piezocomposite actuators embedded in slender structures", in *44th AIAA/ASME/ASCE/AHS/ASC Structures, Structural Dynamics, and Materials Conference* (Norfolk, VA, 2003), AIAA, Reston, VA, 2003. AIAA 2003-1803.

[Cesnik and Shin 1998] C. E. S. Cesnik and S. J. Shin, "Structural analysis for designing rotor blades with integral actuators", in *39th AIAA/ASME/ASCE/AHS/ASC Structures, Structural Dynamics, and Materials Conference* (Long Beach, CA, 1998), AIAA, Reston, VA, 1998. AIAA 1998-2107.

[Cesnik et al. 2001] C. E. S. Cesnik, S. J. Shin, and M. L. Wilbur, "Dynamic response of active twist rotor blades", *Smart Mater. Struct.* **10**:1 (2001), 62–76.

[Cesnik et al. 2003] C. E. S. Cesnik, R. S. Park, and R. Palacios, "Effective cross-section distribution of anisotropic piezocomposite actuators for wing twist", pp. 21–32 in *Smart structures and materials 2003: smart structures and integrated systems* (San Diego, CA), edited by A. M. Baz, Proceedings of SPIE **5056**, SPIE, Bellingham, WA, 2003.

[Esmailzadeh and Ghorashi 1997] E. Esmailzadeh and M. Ghorashi, "Vibration analysis of a Timoshenko beam subjected to a travelling mass", *J. Sound Vib.* **199**:4 (1997), 615–628.

[Esmailzadeh et al. 1995] E. Esmailzadeh, M. Ghorashi, and B. Mehri, "Periodic behavior of a nonlinear dynamical system", *Nonlinear Dynam.* **7**:3 (1995), 335–344.

[Ghorashi 1994] M. Ghorashi, *Dynamic and vibratory analysis of beams under dynamic loads induced by traveling masses and vehicles*, Ph.D. thesis, Mechanical Engineering Department, Sharif University of Technology, 1994.

[Ghorashi 2009] M. Ghorashi, *Dynamics of elastic nonlinear rotating composite beams with embedded actuators*, Ph.D. thesis, Mechanical and Aerospace Engineering Department, Carleton University, 2009.

[Ghorashi and Nitzsche 2008] M. Ghorashi and F. Nitzsche, "Steady state nonlinear dynamic response of a composite rotor blade using implicit integration of intrinsic equations of a beam", *Int. Rev. Aerospace Eng.* **1** (2008), 225–233.

[Hodges 2006] D. H. Hodges, *Nonlinear composite beam theory*, Progress in Astronautics and Aeronautics Series **213**, AIAA, Reston, VA, 2006.

[Hodges et al. 1992] D. H. Hodges, A. R. Atilgan, C. E. S. Cesnik, and M. V. Fulton, "On a simplified strain energy function for geometrically nonlinear behavior of anisotropic beams", *Compos. Eng.* **2**:5–7 (1992), 513–526.

[Palacios 2005] R. Palacios, *Asymptotic models of integrally-strained slender structures for high-fidelity nonlinear aeroelastic analysis*, Ph.D. thesis, University of Michigan, 2005.

[Shang and Hodges 1995] X. Shang and D. H. Hodges, "Aeroelastic stability of composite rotor blades in hover", pp. 2602–2610 in *36th AIAA/ASME/ASCE/AHS/ASC Structures, Structural Dynamics, and Materials Conference* (New Orleans, LA, 1995), AIAA, Reston, VA, 1995. AIAA 1995-1453.

[Yu and Hodges 2004] W. Yu and D. H. Hodges, "Elasticity solutions versus asymptotic sectional analysis of homogeneous, isotropic, prismatic beams", *J. Appl. Mech.* (*ASME*) **71**:1 (2004), 15–23.

[Yu et al. 2002a] W. Yu, D. H. Hodges, V. V. Volovoi, and C. E. S. Cesnik, "On Timoshenko-like modeling of initially curved and twisted composite beams", *Int. J. Solids Struct.* **39**:19 (2002), 5101–5121.

[Yu et al. 2002b] W. Yu, V. V. Volovoi, D. H. Hodges, and X. Hong, "Validation of the variational asymptotic beam sectional analysis", *AIAA J.* **40**:10 (2002), 2105–2112.

[Zwillinger 1998] D. Zwillinger, *Handbook of differential equations*, 3rd ed., Academic Press, San Diego, CA, 1998.

Received 22 Aug 2008. Revised 15 Mar 2009. Accepted 13 May 2009.

MEHRDAAD GHORASHI: mghoras2@connect.carleton.ca
Department of Mechanical and Aerospace Engineering, Carleton University, 1125 Colonel By Drive, Ottawa, ON K1S 5B6, Canada

FRED NITZSCHE: fred_nitzsche@carleton.ca
Department of Mechanical and Aerospace Engineering, Carleton University, 1125 Colonel By Drive, Ottawa, ON K1S 5B6, Canada